The Current Status of the Lepton g Factors

ARTHUR RICH, JOHN C. WESLEY*
Physics Department, University of Michigan, Ann Arbor, Michigan

The past three years have seen new measurements of the g-factor anomalies of the free leptons ($e^{\pm}$, $\mu^{\pm}$). At the same time there have been several major theoretical advances including a quantum electrodynamic calculation of the sixth-order coefficient of the electron anomaly. In this article we review these recent developments in detail, however we also: (1) present a historical overview of g-factor measurements and their interpretation since the early days of quantum theory, (2) discuss several experiments which are currently being attempted but which have not yet yielded results of high precision, (3) attempt to predict the most likely course of g-factor research in the near future. An extensive Bibliography and Tables summarizing both historical events and current work are included.

CONTENTS

INTRODUCTION

As the title of this review indicates, we will devote a major portion of our attention to a discussion of the current status of the g factors of the charged leptons (e^+, e^-, μ^+, μ^-). However, we have also included material of an historical nature, as well as speculation on the possibilities for future progress in the field.

More specifically, this article consists of four major sections. The first section is in the form of an historical narrative from 1920 to the present, discussing past activity related to the calculation and measurement of lepton g factors. In addition to the purely historical material, basic definitions and comments of didactic interest are included at appropriate points. An extensive historical table and a bibliography of literature relevant to the calculation and measurement of lepton g factors will be found in the Appendices. The second section consists of an outline of the application of quantum electrodynamics (QED) to the calculation of lepton g factors, and a discussion of possible modifications of QED and their effect on lepton anomalies. The third and largest section contains a discussion of techniques and experiments of current interest, with major emphasis placed on the basic techniques, rather than on details of specific experiments. Where possible, we have attempted to point out interrelations between apparently dissimilar experiments. A tabulation of experimental results to date is included. For those readers with a more critical interest in precision measurement, we also point out areas of difficulty in each experiment, and appraise the significance of the results. In the concluding section, we summarize the current status of lepton g factors, and assess the potential for future progress in the field.

SYMBOLS AND DEFINITIONS

The cgs system of units will be used throughout this review, except in Chap. II, where we use $\hbar=c=1$. The following symbols will be employed:

Electron charge	e
Electron rest mass	m_e
Muon rest mass	m_μ
Velocity of light	c
Electron magnetic moment	μ_e
Muon magnetic moment	μ_μ
Proton magnetic moment	μ_p
Proton magnetic moment, measured in H_2O, uncorrected for diamagnetism	μ_p'
Bohr magneton	$\mu_B=e\hbar/2m_ec$
Fine-structure constant	$\alpha=e^2/\hbar c\approx 1/137$
Electron g factor	g_e
Muon g factor	g_μ
Atomic g factor	g_J
Electron g factor anomaly	$a_e=(\lvert g_e\rvert-2)/2$
Muon g factor anomaly	$a_u=(\lvert g_\mu\rvert-2)/2$

* Present address: Department of Physics, Yale University, New Haven, Connecticut 06520.

I. HISTORY AND DEFINITIONS

1.1 Definitions and PreQED History

For an elementary particle with mass M, charge Q, and intrinsic angular momentum (spin) $\mathbf{S}$, symmetry requires that any associated magnetic moment $\boldsymbol{\mu}$ be parallel or antiparallel to $\mathbf{S}$. Dimensional analysis shows that $\boldsymbol{\mu}$ will be proportional to $(Q/Mc)\mathbf{S}$. Expressed as an equality, this relation becomes

$$\boldsymbol{\mu}=(g/2)(Q/Mc)\mathbf{S}, \tag{1.1}$$

where the constant of proportionality g (the g factor) is dimensionless.[1] Dividing g by 2 is conventional. The magnitude of g is characteristic of the internal structure or interactions of the particle. The degree of agreement between theoretical predictions and experimental measurements of g therefore provides a means for testing the validity of the theory.

Historically, the earliest approach to calculation of a lepton g factor was to treat the electron as a charged rigid spinning object of finite dimensions. The spinning charge gives rise to equivalent current loops, so that if the charge distribution and spin are known, the magnetic moment can be calculated from elementary considerations. For a body with charge density $\rho_e(r)$ and mass density $\rho_m(r)$, the g factor is determined by the functional dependence of the ratio ρ_e/ρ_m. If this ratio is constant throughout the body, then $g=1$ regardless of the geometrical shape of the object. Also, for the case of an electron in a circular orbit, the orbital g factor is equal to unity.

The earliest speculations on the intrinsic spin and magnetic moment of the electron were based on indirect experimental evidence. In 1921, Compton noted that the phenomenon of ferromagnetism appeared to be associated with an intrinsic magnetic moment of the electron, rather than with the orbital moment of electrons in an atom or molecule, and that the magnitude of ferromagnetic effects seemed to require an effective charge-to-mass ratio substantially greater than e/m_e, i.e., in current terminology, an electron g factor substantially greater than unity. Compton pointed out that a g factor greater than unity could be obtained by assuming that the electron was a spinning object of finite dimensions, with the electron mass more centrally concentrated than the electron charge. Furthermore, Compton noted that an electron spin of approximately h would account for the necessary magnetic moment. Although the reasoning that lead Compton to some of his conclusions was erroneous, he seems to have been the first to propose an electron with intrinsic spin and magnetic moment in order to explain a specific effect.

In 1925 Uhlenbeck and Goudsmit were able to make more quantitative speculations about the intrinsic properties of the electron. By postulating that the electron had a spin of $\frac{1}{2}\hbar$ and $g=2$, they were able to use the Bohr–Sommerfeld quantum theory to explain the optical doublets and the anomalous Zeeman effect in alkali spectra. Further calculation of the consequences of these postulates by other workers soon led to a satisfactory understanding of many previously unexplained phenomena. Within two years, Dirac (1927) was able to show that $S=\hbar/2$ and $g=2$ followed from a covariant formulation of Schrödinger's quantum theory.

Following its introduction, the Dirac theory enjoyed great success in predicting many phenomena of atomic physics. However, by 1947 experiments of increasing accuracy began to reveal small but significant discrepancies from the predictions of the Dirac theory. In 1947, Lamb and Retherford discovered the Lamb shift by showing that the $2^2S_{1/2}$ and $2^2P_{1/2}$ states of hydrogen were separated by about 1000 MHz, instead of being degenerate, as predicted by Dirac. Also in 1947, Nafe, Nelson, and Rabi obtained precision measurements of the hyperfine structure intervals in hydrogen and deuterium. They noted that their measurements showed a 0.2% discrepancy from predictions of the hyperfine structure interval based on $g=2$. These experiments indicated that the Dirac theory of the electron was no longer completely satisfactory, and thus set the stage for the introduction of the current theory of quantum electrodynamics.

1.2 Lepton g Factors and QED: History II

Since 1947, measurements of lepton g factors have been closely associated with the development of QED. From 1947 to the present, the precision of both theoretical calculation and experimental measurement has improved by six orders of magnitude (see Figs. 1.1 and 1.2). One of the most striking features of this improvement has been an almost exact correspondence between the accuracy of theory and experiment. The past 24 years have seen a continuing series of confrontations between theory and experiment at ever increasing levels of precision. This close interaction between theory and experiment has undoubtedly been a strong stimulus to both areas.

The first experimental evidence that the g factor differed slightly from two was contained in the hyperfine structure measurements of Nafe, Nelson, and Rabi, reported in May 1947. In September of the same year, Breit proposed that the discrepancy could be attributed to a correction of order α to the Dirac g factor. In November 1947, Kusch and Foley reported the first

[1] The concept of a scalar g factor requires that certain restrictions be placed on the theory or model assumed to describe the particle. For instance, a tensor g factor may be required for a nonrigid spinning classical electron. For a quantum mechanical Dirac (spin $\frac{1}{2}$) particle, the only vector operator available is the Pauli spin operator $\boldsymbol{\sigma}$ so all vector quantities, including $\boldsymbol{\mu}$, must be proportional to $\mathbf{S}=\frac{1}{2}\hbar\boldsymbol{\sigma}$.

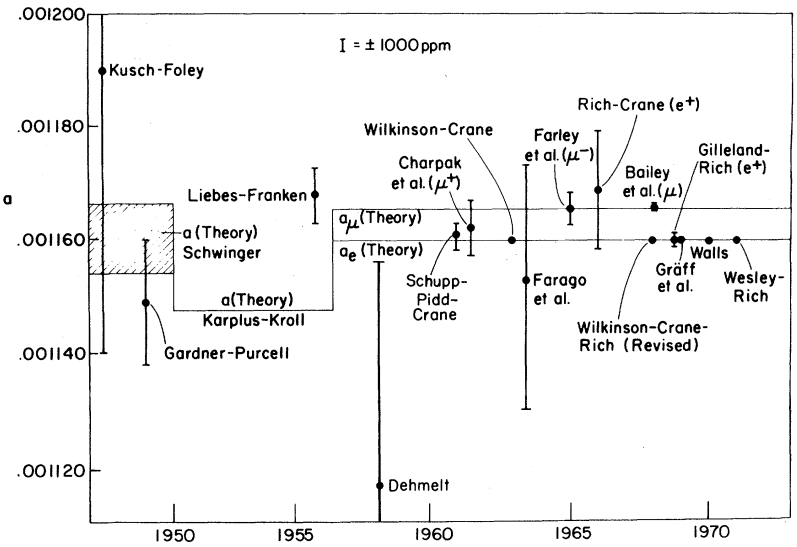

FIG. 1.1. Theoretical and experimental determinations of the lepton g-factor anomalies.

direct measurement of the electron g factor. With the g-factor anomaly a defined as $(|g|-2)/2$, their result could be expressed as $a_e^-=0.00119(5)$.[2] By December 1947, Schwinger was able to develop a nondivergent formulation of QED that permitted him to show that the lowest-order radiative correction to the electron anomaly was equal to $\alpha/2\pi(=0.00116)$. Schwinger's application of the concepts of mass and charge renormalization [first suggested by Kramers (1947)] provided the key to eliminating the divergences that led to the failure of previous theories of QED.[3] Although the renormalization aspects of the theory are considered by many to be unsatisfying esthetically, as we will see, the practical success of the theory is undeniable.

In 1949, Dyson showed that Schwinger's theory could be extended to permit calculation of higher-order corrections to the properties of quantum systems. By showing the equivalence of the Schwinger–Tomonaga and Feynman formulations of the theory, Dyson was able to simplify the calculational procedure, devise an unambiguous program for obtaining the nth-order contribution to quantities which can be calculated using QED, and show that these contributions would remain finite to arbitrary order in α. Thus, for example we have

$$a_e=A_e(\alpha/\pi)+B_e(\alpha/\pi)^2+C_e(\alpha/\pi)^3+\cdots. \quad (1.2)$$

Schwinger's calculation was therefore equivalent to $A_e=\frac{1}{2}$. Dyson was careful to note that the existence of finite coefficients in expansions of the type given in Eq. (1.2) does not necessarily imply convergence of the series. The question as to whether QED diverges, converges absolutely, or only converges asymptotically remains unanswered at the present time (see Sec. 2.2).

The inherent divergences of QED make intuitive interpretation of the theory difficult. Several theorists, including Luttinger (1948), Welton (1948), and Koba (1949) attempted to calculate a for special quantum states, or by semiclassical approximations. Welton obtained $a_e=-\alpha/2\pi$, while Koba was able to refine the semiclassical method sufficiently to obtain the correct result of $a_e=\alpha/2\pi$. These attempts were useful in providing an intuitive explanation for the existence of a, but the techniques proved to be of no further use in more precise calculations.

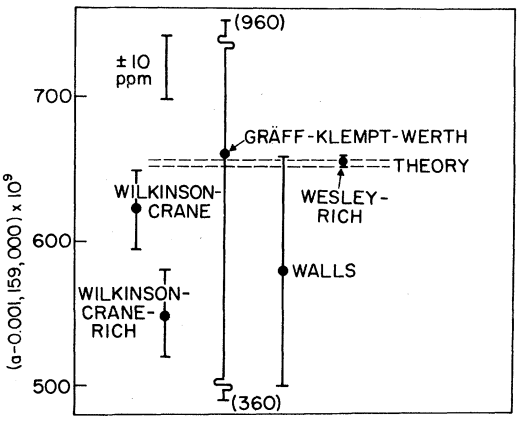

FIG. 1.2. Recent electron g-2 measurements.

[2] The quantity enclosed in parentheses represents the uncertainty in the final digits of a numerical value. Thus, 0.00119(5) is equivalent to 0.00119±0.00005. All errors are one standard deviation, unless otherwise noted.

[3] The first use of the renormalization concept was in a nonrelativistic calculation of the Lamb shift by Bethe (1947). Schwinger was the first to treat the problem of the Lamb shift and the electron anomaly using a relativistic formulation. The theory of QED was also developed independently by Tomonaga (1946) and Feynman (1948).

In 1950, Karplus and Kroll reported a calculation of the second-order contribution to a_e. Their result was $B_e = -2.97$. However, in 1956, a precision measurement of g_e^- by Liebes and Franken (see below) suggested a significantly different value for B_e. Recalculations of the fourth-order coefficient by Sommerfield (1957) and Petermann (1957) revealed that a portion of the Karplus–Kroll calculation was in error. The revised value is

$$B_e = (197/144) + (\pi^2/12) + \tfrac{3}{4}\zeta(3) - \tfrac{1}{2}\pi^2 \ln 2 = -0.32848\ldots \quad (1.3)$$

(ζ is the Riemann Zeta function).

In 1949, Gardner and Purcell introduced a technique that eventually permitted measurements of g_e^- to approximately 1 ppm. Their method was based on a comparison of the cyclotron frequency of free electrons to the NMR frequency of protons, and thus provided a precision value for μ_p/μ_B. When this value was combined with measured values of μ_e/μ_B, the resulting value of a_e^- provided further confirmation of the results of Schwinger and Kusch and Foley. Further refinements of the technique by Franken and Liebes (1956) and Hardy and Purcell (1958) resulted in determinations of a_e^- to approximately 1000 ppm, permitting a preliminary test of QED through second order in α. For instance, the result of the Liebes–Franken experiment can be expressed as[4]

$$a_e^-(\text{expt}) - 0.5(\alpha/\pi) = (1.2 \pm 0.9)(\alpha/\pi)^2. \quad (1.4)$$

As noted above, this result provided an important stimulus for the theoretical calculations of Sommerfield and Petermann in 1957.

The various experiments mentioned above all determined the g factor indirectly, either from atomic g_J values, or from a comparison of electron and proton resonance frequencies. The inherent accuracy of the first type of experiment is limited to approximately 10^3 ppm of a by uncertainties in the spin–orbit theory necessary to obtain g_e from g_J (Kusch and Foley, 1948). Careful experiments of the second type can also reach accuracies of about 1000 ppm of a (Klein, 1968), barely sufficient to test QED to second order. For a precision determination of a, it is highly desirable to: (1) measure a (i.e., g-2) directly, and (2) make such a measurement on free electrons, so as to avoid the corrections necessary to account for atomic binding effects.

The first direct measurement of the g factor of free electrons was made by Louisell, Pidd, and Crane at the University of Michigan in 1953. Although their final result of $g_e^- = 2.00 \pm 0.01$ was not accurate enough to determine the anomaly, the experiment did demonstrate that it was possible to measure the g factor of free electrons. Bohr had pointed out (see Pauli, 1933) that an attempt to measure the magnetic moment of a free particle by means of a change in the classical trajectory of the particle (i.e., by a Stern–Gerlach type experiment) would violate the uncertainty principle, since it would require a simultaneous measurement of the particle's position and momentum. Other writers interpreted this argument as implying that the magnetic moment of a free particle could not be measured in any way, and was therefore a meaningless concept (see Mott and Massey, 1965). In fact, a Stern–Gerlach determination of g is possible if one performs the experiment in a statistical fashion; that is, by sending many particles through the apparatus and making a detailed study of the line shape (see Louisell, Pidd, and Crane, 1953, for a discussion of this point). The uncertainty principle does show that the splitting of the trajectory due to the magnetic moment will be small compared to the linewidth, and that an actual measurement by this method is not practical.

The method actually employed by the Michigan group to measure g_e consisted of a Mott double-scattering experiment, with a uniform magnetic field separating the initial and final scatterings. The magnitude of g was determined by measuring the rotation of the electron spin between the scatterings. The method thus requires a simultaneous measurement of the electron position and a single component of **S**, which in no way violates the uncertainty principle. In 1961, Schupp, Pidd, and Crane reported an improved version of this technique, in which, instead of measuring the total spin rotation between scatterings, they arranged to measure only the differential rotation of the spin with respect to the electron velocity. Since the frequency of this so-called g-2 precession is directly proportional to the anomaly (Sec. 3.1.1), a direct g-2 measurement was possible. The magnetic field used in the experiment was in the form of a magnetic mirror trap, which permitted the electrons to undergo several hundred g-2 precessions between scatterings. The initial accuracy of the Schupp experiment was 2100 ppm of a, with a result:

$$a_e^-(\text{expt}) - 0.5(\alpha/\pi) = (-0.09 \pm 0.44)(\alpha/\pi)^2.$$

This again confirmed the recalculated value of B_e, but fell somewhat short of a definitive check. Further improvement of the Michigan g-2 technique by Wilkinson and Crane (1963) permitted sufficient experimental accuracy for a precision check of B_e. The original experimental result, expressed in terms of the then current value of $\alpha[\alpha^{-1} = 137.0391(5)]$ was

$$a_e^-(\text{expt}) - 0.5(\alpha/\pi) = (-0.327 \pm 0.005)(\alpha/\pi)^2. \quad (1.5)$$

The excellent agreement between the Wilkinson–Crane result and the Sommerfield–Petermann calculation

[4] To permit the comparison of experimental results with theory, we will express them in the form of Eq. (1.4). The precise value of the coefficient on the right-hand side will depend on the value of α used. Unless otherwise noted, we will use the currently accepted value of $\alpha[\alpha^{-1} = 137.03608(26)]$, as recommended by Taylor, Parker, and Langenberg (1969). Except for measurements of a to accuracies of better than 50 ppm, the precise value of α used is not significant.

was widely interpreted as a definitive test of the application of QED to the calculation of the electron anomaly. As we will note at a later point in this discussion, subsequent revision of the theoretical value of a_e owing to changes in α and refined analysis of the original Wilkinson–Crane data led to an apparent "disagreement" between theory and experiment that has only recently been resolved.

During the period of the development of the Michigan experiments, other workers proposed or developed alternate means to measure g or a for free electrons. An experiment by Farago, Gardner, Muir and Rae (1963) employed a variation of the Schupp–Pidd–Crane technique to measure a_{e^-} to 2%. In 1953, Bloch proposed a novel resonance-type experiment to measure g_e using electrons occupying the lowest Landau level in a magnetic field. This proposal eventually became the basis for the experiment currently being carried out at Stanford by Fairbanks and co-workers. In 1958, Dehmelt demonstrated that spin–exchange collisions between oriented sodium atoms and free, thermal energy electrons could be used to measure g_e via a direct RF-resonance technique. As a means of illustrating the precision of the technique, Dehmelt (1958) reported a measurement of $g_e/g_j(\mathrm{Na})$ accurate to 30 ppm. Since, at that time, $g_j(\mathrm{Na})$ was known to an accuracy of about 20 ppm, Dehmelt's result implies $a_{e^-}=0.001116(40)$, and thus constitutes the first measurement of a for free electrons. Experiments of a related, but somewhat different nature are currently being carried out at the University of Washington by Dehmelt (1968) and co-workers, and at Johannes Gütenberg University in Mainz by Gräff and co-workers (1969). At the present time, none of these methods has reached the accuracy of the Schupp–Pidd–Crane technique (see Secs. 3.2.2 and 3.2.3).

In addition to the various measurements of the electron anomaly, the Michigan group has also extended their technique to measurements of the positron g factor. Since the TCP theorem requires that particle and antiparticle have equal mass, and equal but opposite charge and magnetic moment, a comparison of the electron and positron g factors provides a direct test of the consequences of TCP invariance. The original measurement of a_{e^+} by Rich and Crane in 1966 was followed by an improved measurement by Gilleland and Rich in 1969. Both experiments employed a modified version of the Schupp–Pidd–Crane g-2 technique. The final result of the Gilleland–Rich experiment shows that the positron anomaly agrees with the electron anomaly to 1000 ppm, and hence that $g_{e^+}=g_{e^-}$ to 1 ppm. It is interesting to note that for electrons, the accuracy to which the g factors have been compared is approximately 100 times greater than the accuracy to which $(e/m_e)_{e^+}$ and $(e/m_e)_{e^-}$ have been compared.

At this point in the discussion, let us turn our attention to the "anomalous" leptons, the μ mesons, or muons. The known interactions of the muon are identical to those of the electron, yet the muon mass is approximately 200 times the electron mass. Since current elementary particle theories are based on the concept that a particle's mass is a characteristic of its interactions, the cause of the $\mu-e$ mass difference remains an enigma. It is hoped that a detailed investigation of the static properties of the muon (such as the magnetic moment) will help in clarifying this puzzle. Accordingly, considerable effort has been devoted to calculation and measurement of the muon g factor. By 1957, Suura and Wichman (1957) and Petermann (1957) had calculated the difference between the electron and muon anomalies through order $(\alpha/\pi)^2$. Recently, Brodsky and Kinoshita (1970) have completed a calculation of the electromagnetic contributions to the anomaly difference through terms of order $(\alpha/\pi)^3$. The combined result of these calculations is

$$a_\mu-a_e=1.09426(\alpha/\pi)^2+(20.3\pm1.3)(\alpha/\pi)^3. \quad (1.6)$$

The difference between a_μ and a_e is due to a dependence of vacuum polarization effects on the lepton mass (see Sec. 2.1). Strong interactions also affect lepton anomalies via the vacuum polarization contributions of the neutral vector bosons. This effect is appreciable (50 ppm) only for the muon anomaly (see Sec. 2.1). The contribution to a can be related to the total cross section for vector boson production in $e^-—e^+$ interactions. Gourdin and de Rafael (1969) find, on the basis of the Orsay colliding beam data, that the hadronic vacuum polarization contribution from the ρ, ω, and ϕ resonances is

$$(\delta a_\mu)_{\mathrm{strong}}=(6.5\pm0.5)\times10^{-8}. \quad (1.7)$$

This is equivalent to $(5.2\pm0.4)(\alpha/\pi)^3$. The total difference between a_μ and a_e is approximately 0.6% of a.

The initial measurement of g_μ by Coffin *et al.* (1958) was obtained by measuring the spin precession frequency of stopped muons in a known magnetic field. This procedure yields an absolute value for μ_μ. In order to obtain g_μ, the muon magneton $e\hbar/2m_\mu c$ is required. Although the precession frequency can be measured to about 10 ppm, uncertainty in m_e/m_μ limits the accuracy of g_μ to about 100 ppm. Therefore, this method is limited to an accuracy of about 10% of a_μ, and hence cannot be used to check for muon—electron differences.

A direct determination of a_μ avoids the necessity of knowing m_μ/m_e. In fact, combining the results of the precession experiments with a value for g_μ leads to a more accurate value for m_μ/m_e. The first direct measurement of a_{μ^+} by Charpak *et al.* at CERN reached an accuracy of 2% of a_μ in 1961, and with further improvements, a final accuracy of $\frac{1}{2}$% of a_μ in 1965. As in the electron experiments of Crane *et al.*, the anomaly was determined from a measurement of the relative precession of the muon spin with respect to the velocity, for muons confined in a nearly homogeneous magnetic field. In the case of Charpak's experiment, the muons were confined by precisely controlled gradient drift in a

long linear magnet. In further refinements of this method by Farley *et al.* (1966) and Bailey *et al.* (1968), the linear magnet was replaced by a muon storage ring in order to increase the total g-2 precession angle of the trapped muons. The 1968 measurement reached an accuracy of 270 ppm of a_μ. Although some disagreement between preliminary estimates of a_μ and the results of the CERN experiment was reported in an initial account of the experiment (Bailey *et al.*), subsequent calculation of the sixth-order electron—muon anomaly difference contributions and the effect of hadronic vacuum polarization now results in good agreement between theory and experiment. The CERN experiment also shows that $g_{\mu^+}=g_{\mu^-}$ to 0.7 ppm, thereby providing a test of TCP invariance.

Returning to the electron, we note that by 1969, the initial agreement between the Wilkinson–Crane experiment and theory had been transformed into a significant discrepancy. Several systematic errors were present in the original data analysis of Wilkinson and Crane. Correction of these errors lowered the experimental result by approximately two standard deviations (Rich, 1968; Henry and Silver, 1969). At about the same time, measurements of the fine-structure constant obtained by using the ac Josephson effect indicated that the previously accepted value of α was incorrect. The revised Wilkinson-Crane result, expressed in terms of the new value for α $[\alpha^{-1}=137.03608(26)]$ was

$$a_{e^-}(\text{expt})-0.5(\alpha/\pi)=(-0.344\pm0.005)(\alpha/\pi)^2, \tag{1.8}$$

or alternately,

$$a_{e^-}(\text{expt})-[0.5(\alpha/\pi)-0.32848(\alpha/\pi)^2]=(-7.0\pm2.4)(\alpha/\pi)^3. \tag{1.9}$$

The experimental value for C_e in Eq. (1.9) was difficult to reconcile with the dispersion theory estimates of Drell and Pagels (1965) and Parsons (1968), which suggested that C_e was of order 0.1. This discrepancy, in combination with similar discrepancies found in measurements of the Lamb shift in hydrogen and helium, led to considerable interest in a possible breakdown of QED (see Taylor, Parker, and Langenberg, 1969).

Fortunately (or unfortunately, depending on your point of view), these discrepancies appear to have been resolved. Recent Lamb shift measurements are now in excellent agreement with QED theory. At the present time, the electron anomaly is also in agreement with QED predictions to order $(\alpha/\pi)^3$. The final result of a high-field electron g-2 measurement at Michigan by Wesley and Rich (1971) is

$$a_{e^-}(\text{expt})-[0.5(\alpha/\pi)-0.32848(\alpha/\pi)^2]=(1.68\pm0.33)(\alpha/\pi)^3. \tag{1.10}$$

This value is in good agreement with the recently completed exact evaluation of vertex contributions to C_e by Levine and Wright (1971), which, in combination with other contributions previously calculated by Mignaco and Remiddi (1969), Aldins *et al.* (1970), and Brodsky and Kinoshita (1970) yields $C_e=(1.49\pm0.2)$.

Very recently, Ford and Granger (1971) have completed a comprehensive analysis of the spin-motion theory used to interpret the Michigan experiments (see Sec. 3.1.2). They find that further corrections to the Wesley–Rich and revised Wilkinson–Crane values are necessary. In the case of the Wesley–Rich value, the revision is small (about one standard deviation). For the Wilkinson–Crane value, the correction is large, and apparently brings the final result into satisfactory agreement with both Wesley–Rich and current theory.

The agreement noted above should be treated with a certain amount of caution, since it is based on a comparison between a single theoretical calculation and a single type of experimental measurement. In view of the complexities of the theoretical calculation, and the difficulty of accurately estimating the systematic errors associated with a specific experiment, independent checks of both theory and experiment are of great importance. There are, to our knowledge, at least six theoretical groups now working on calculations of the sixth-order anomaly contributions. Hopefully, further checks of current calculations will be available in the near future. On the experimental side, it appears possible that the resonance experiments currently in progress at Washington, Mainz, and Stanford may yield measurements of a_{e^-} at the 10 ppm level (or better) within the next few years. Proposed muon experiments (Sec. 4.3) may also permit an order of magnitude increase in accuracy in measurements of a_μ. It is quite possible that in the new few years we will see a definitive test of QED through order $(\alpha/\pi)^3$ for both electrons and muons.

II. QED THEORY AND LEPTON ANOMALIES

One of the outstanding successes of QED has been the accurate prediction of lepton g-factor anomalies. Indeed, the agreement between the experimental measurements and QED predictions of the electron g factor at a level of four parts per billion represents the most accurate comparison between theory and experiment in physics. In spite of the unsatisfactory nature of the renormalization aspects of the theory, there has been no significant evidence for a breakdown of QED, at least within the range of energies and momentum transfers explored. In this chapter, we will attempt to outline the application of QED to g-factor calculations, and the possible effects of a breakdown of the theory on the anomalies of the charged leptons. For an extensive analysis of the current situation, the reader is directed to reviews by Farley (1969), Brodsky, and Drell (1970) and Lautrup, Petermann, and de Rafael (1971). The possibility that the neutrino may have a magnetic

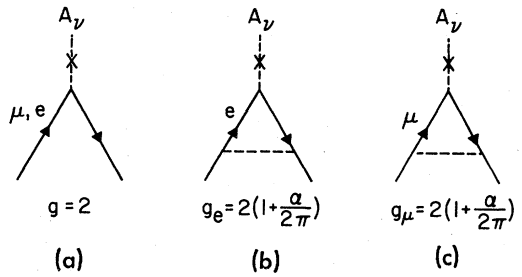

FIG. 2.1. Second-order corrections to the lepton g-factors.

moment, and some astrophysical consequences of this possibility, have been considered by Cisneros (1970).

2.1 Calculation of Lepton Anomalies

There have been two alternate approaches to the formulation of QED and the application of this formalism to calculation of the properties of quantum systems. These are the "Feynman diagram" method, and the "mass operator" method. Since the first method provides a more intuitive description of the physical processes which can be thought of as giving rise to the anomalous moment, we will begin with it.

2.1.1 *The Feynman Diagram Method*

The interaction of an electron with an external field A_ν ($\nu=1, 2, 3, 4$) can be represented by the Feynman diagram (graph) shown in Fig. 2.1(a). The interaction is that described by the Dirac Hamiltonian; the corresponding g factor is exactly 2. There is, in addition, a small probability that the electron will emit and reabsorb a virtual photon during the course of its interaction with the external field, as shown in Fig. 2.1(b). This process alters the interaction energy of the electron with the (external) magnetic field, and thus gives rise to a corresponding correction to the g factor. Figure 2.1(b) represents the simplest possible self-interaction; obviously, more complex diagrams, involving multiple virtual photons (and lepton–antilepton pairs) are also possible. It can be shown (Dyson, 1949) that treating the problem in terms of Feynman diagrams is formally equivalent to a perturbation theory calculation of the interaction energy. Summing over all possible diagrams containing $2n$ internal (virtual) vertices yields the $2n$th-order perturbation theory contribution, proportional to e^{2n} (recall that since $\hbar=c=1$, $e^2=\alpha$). The $2n$th-order contribution is expected to be of order α^{2n} if the series converges or if we are in the valid domain of an asymptotic expansion. Consequently, evaluation of the first few terms in the power series expression should (in principle) be sufficient to yield a value for the anomaly accurate to several parts per million.

By employing the "rules" of QED (see, for example, Feynman, 1961) each diagram can be used to construct an integral expression for the interaction energy arising from the process depicted. Those terms which are linear in A_ν correspond to the contribution of the anomalous magnetic moment. Integration over the Feynman parameters, parameters introduced to carry out integration with respect to the momenta of the virtual particles, leads to a numerical answer for each diagram. Proper application of renormalization concepts is required both on physical grounds and to avoid the divergences that occur if a straightforward evaluation of the integral expression is attempted.

The second-order diagram for the muon anomaly is shown in Fig. 2.1(c). For diagrams involving only virtual photons, the respective contribution to the anomaly is independent of the type of lepton. As noted in the following paragraph, differences between the electron and muon anomalies arise only in diagrams that contain both types of particles.

The computational procedure can be extended to higher orders. Figure 2.2 shows the eight (six independent) possible fourth-order diagrams. Diagrams 2.2(e) and 2.2(f) describe the phenomena of vacuum polarization, in which a photon creates a lepton–antilepton pair that subsequently annihilates to reform the photon. Since a process of this type requires a minimum of four vertices, it is possible only in fourth- and higher orders. Because of the increased number of virtual particles, additional integrations are necessary. Analytic interpretation is difficult, but feasible. The contributions of the various diagrams are given in Fig. 2.2. Note that, in principle, electron and muon pairs (loops) contribute to both a_e and a_μ [Figs. 2.2(e) and 2.2(f)]. The contribution of electron pairs to a_e and the contribution of

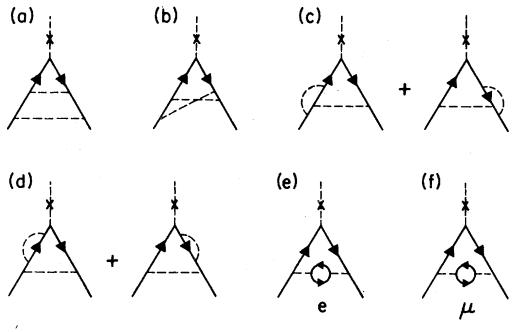

Graph	$\delta a_e/(\alpha/\pi)^2$	$\delta a_\mu/(\alpha/\pi)^2$
(a)	0.778	0.778
(b)	-0.467	-0.467
(c)	-0.564	-0.564
(d)	-0.09	-0.09
(e)	0.016	1.094
(f)	$\sim 10^{-6}$	0.016

FIG. 2.2. Fourth-order graphs and contributions to a_μ and a_e.

muon pairs to a_μ are identical. The contribution of muon pairs to a_e has been calculated (Lautrup and de Rafael, 1968) to be $(1/45)(\alpha/\pi)^2(m_e/m_\mu)^2$ or about 10^{-6} $(\alpha/\pi)^2$. It is therefore negligible in comparison to other fourth-order contributions. On the other hand, the contribution of electron pairs to a_μ is $1.09(\alpha/\pi)^2$, and is primarily responsible for the difference between a_e and a_μ.

Vacuum polarization contributions are not limited to those from lepton loops. Virtual hadrons can also contribute, by the process shown in Fig. 2.3(a), where the components of the loop consist of various hadronic pairs, such as $\pi^+-\pi^-$, K^+-K^-, p^+-p^-, etc. Since these particles interact strongly, the internal composition of the loop is very difficult to analyze. However, by applying dispersion theory, one can "cut" Fig. 2.3(a) in half, giving Fig. 2.3(b), which describes the production of real (nonvirtual) hadrons. Consequently, it is possible to relate the total cross section for hadron production in e^+-e^- scattering to the effect on the anomaly (see Farley, 1969). The cross section is dominated by the ρ, ω, and φ resonances, so that one is perhaps justified in thinking of the hadronic loop as being effectively composed of a combination of ρ, ω, and φ mesons [Fig. 2.3(c)]. The contribution of each resonance to a_μ, viz $\delta^\rho a_\mu$ etc., has been evaluated by Gourdin and de Rafael (1969):

$$\delta^\rho a_\mu = (5.4\pm0.3)\times10^{-8},$$
$$\delta^\omega a_\mu = (0.61\pm0.12)\times10^{-8},$$
$$\delta^\varphi a_\mu = (0.50\pm0.08)\times10^{-8}.$$

The total contribution is $(6.5\pm0.5)\times10^{-8}$ which is equivalent to $(0.012\pm0.001)(\alpha/\pi)^2$, or $(5.2\pm0.4)(\alpha/\pi)^3$. Thus the hadronic contribution is comparable to the fourth-order muon vacuum polarization contribution. The contribution of hadronic vacuum polarization to a_e will be of order $(m_e/m_\mu)^2$ times that for a_μ, and is therefore entirely negligible in sixth order. Finally, the weak interactions, if mediated by an intermediate boson $(W^\pm)$, can decrease a_μ by about 2×10^{-8} (Brodsky, 1967; Burnett, 1967).

In the past few years, a great deal of attention has been directed towards evaluating the sixth-order contributions to the electron and muon anomalies. The calculational problems are formidable. There are 72

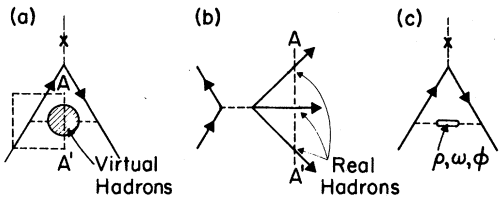

FIG. 2.3. Graphs for calculation of hadronic vacuum polarization contributions.

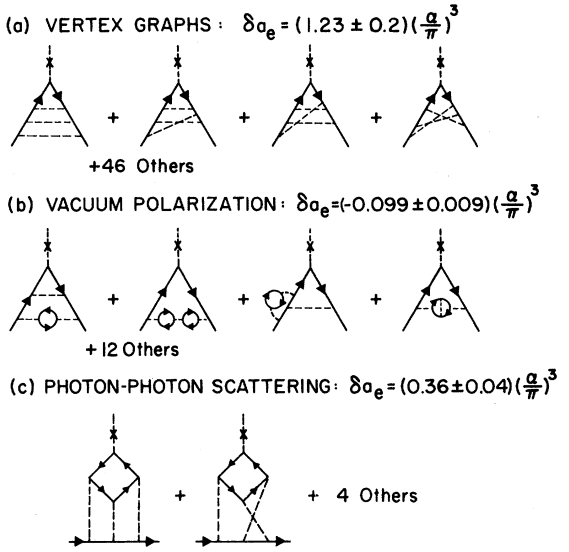

FIG. 2.4. Sixth-order graphs and contributions to the electron anomaly.

distinct diagrams, of the types shown in Fig. 2.4. Sixth-order is marked by the first appearance of the phenomenon of photon–photon scattering [Fig. 2.4(c)]. The integral expressions obtained from the sixth-order diagrams are seven dimensional, and are of such complexity that the algebraic manipulations and integrations required to complete their evaluation in most cases require the use of a digital computer. The necessary Feynman algebra can be handled with algebraic manipulation programs such as REDUCE (Hearn, 1968), and the resultant integrals can be evaluated by a variety of numerical techniques. All sixth-order diagrams have been evaluated. The total sixth-order contribution to a_e is

$$[(1.23\pm0.2)+0.0554-(0.154\pm0.009)+(0.36\pm0.04)]\times(a/\pi)^3=(1.49\pm0.2)(\alpha/\pi)^3.$$

Here the first, and by far the most difficult term to calculate, is the sum of the vertex contributions (Levine and Wright, 1971), the second (Mignaco and Remiddi, 1969) and third (Brodsky and Kinoshita, 1970) terms are vacuum polarization contributions, and the fourth term is the photon–photon scattering contribution (Aldins *et al.*, 1970). The uncertainties are due to the numerical integration procedures used in the evaluation. In principle it should be possible to reduce these errors as much as is desired by improvement of the integration technique. In fact, an increase in precision by perhaps a factor of five is seen as feasible in the near future (Levine, private communication).

2.1.2 *The Mass Operator Method*

Instead of using the Feynman approach discussed above, one can formulate QED in terms of a mass

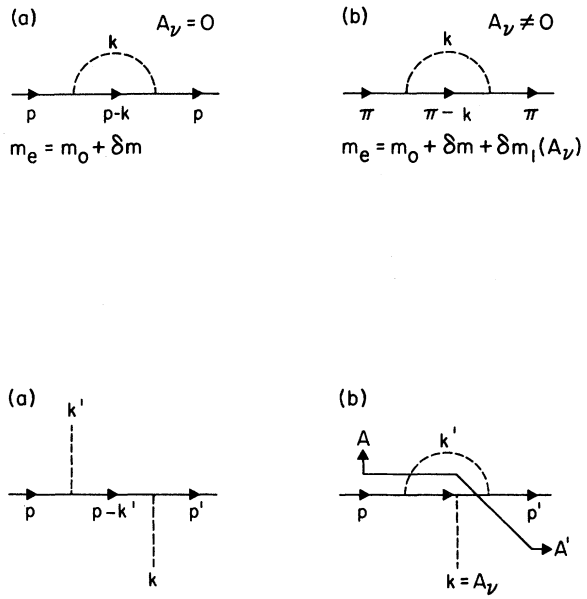

FIG. 2.5. Graphs used for dispersion estimates of the electron anomaly.

operator. Consider a diagram of the type shown in Fig. 2.5(a), which describes the self-interaction of an electron in a field-free region. This diagram leads to the well-known fact that the observable mass of the electron (m_e) is the sum of the "bare" electron mass (m_0), plus a correction δm due to the self-energy of Fig. 2.5(a). One can obtain an integral expression for δm (see Feynman, 1961); however, this expression is logarithmically divergent as k (the momentum of the virtual photon) approaches infinity. This difficulty can be avoided by proper application of the concept of mass renormalization, the details of which need not concern us here. Let us now consider the self-energy of an electron in the presence of an external field A_ν. The effect of this field can be included by replacing the momentum operator p_ν in the electron propagator by the canonical momentum operator $\pi_\nu = p_\nu - eA_\nu$. If the resultant expression for δm is rationalized and expanded, then to lowest order in A_ν, the mass correction can be expressed as the sum of the usual zero-field mass correction, plus a term linear in the external field, viz:

$$\delta m_{\text{total}} = \delta m + \delta m_1(A_\nu) + \cdots .$$

Here $\delta m_1(A_\nu)$ represents the explicit mass correction due to the external field, or in more familiar terms, the change in the rest energy due to the anomalous magnetic moment. The distinction between the mass operator formalism and the Feynman formalism is in the means by which the external field is introduced. In the mass operator method, the field is included indirectly via the lepton propagator, while in the Feynman method, the field is introduced by means of an explicit external vertex. Needless to say, the two methods are conceptually equivalent and should give identical results.

As in the Feynman method, the expressions for the mass operator can be constructed from the corresponding interaction diagram. Expansion to isolate terms linear in A_ν and integration over the Feynman variables leads to a numerical contribution to the anomalous moment. In sixth-order, computer methods are necessary, since the complexity of both the algebra and the integration is comparable to that which occurs in the Feynman method. The principal advantages of the mass operator formalism are that the resultant integral expressions are fewer in number and somewhat simpler, and mass and charge renormalization can be included more readily. Carroll and Yao at Michigan (private communication) are currently working on a calculation of the sixth-order contributions to a_e using the mass operator technique.

2.1.3 *Dispersion Theory Estimates of the Anomaly*

Even in lowest order, the usual approach to QED offers little intuitive insight as to the sign, much less the magnitude of the anomaly. The only way to obtain the desired answer is to carry out the complete calculation. Drell and Pagels (1965) and Parsons (1968) have attempted to employ dispersion theory as a means of estimating the anomaly. Their approach is based on the similarity of the interactions that give rise to the anomaly to those which are involved in Compton scattering. Consider the second-order Compton scattering interaction, as shown in Fig. 2.5(a). If the scattered photon is reabsorbed by the scattered electron, the resultant diagram [Fig. 2.5(b)] is that used to describe the anomaly to second order. Since the probability amplitude for Compton scattering is well known, this information can be used to simplify calculation of the anomaly. If the Klein–Nishina–Compton amplitude is used, Drell and Pagels have shown that the Schwinger term can be obtained exactly. Furthermore, if the effect of the second-order anomalous moment is included in the Compton cross section, a satisfactory approximation to the fourth-order contribution to the anomaly can be obtained by employing an appropriate cutoff of the high-energy contributions to the dispersion integral. Finally, if the fourth-order anomalous moment is included in the Compton cross section, and if the cutoff used in the fourth-order estimate is retained, the sixth-order contribution to the anomaly is found to be approximately 0.15. Brodsky and Kinoshita (1970) have pointed out that the dispersion theory estimate neglects the effects of vacuum polarization and light-by-light scattering, and that it therefore includes only the vertex contributions [Fig. 2.4(a)]. Unfortunately, the agreement between the Drell–Pagels–Parsons estimate and

the exact calculation of the vertex contributions by Levine and Wright is poor. If the exact calculation is confirmed by other workers it would indicate that the approximations made in the dispersion theory calculation of the electron anomaly are unsatisfactory.

2.2 Consequences of a Breakdown of QED

In discussing the motivation for precision measurements of lepton anomalies, the standard answer is that "one is testing the validity of QED." Exactly what one is testing is considerably more difficult to specify. So long as experiment and theory agree, one can assume that the present formulation of QED is satisfactory. If, however, a significant discrepancy is found, the cause of the discrepancy would by no means be unambiguously indicated. A substantial amount of attention has been devoted to hypothetical modifications of QED and the resultant effect on properties of quantum systems. An extensive series of references to calculations of the effects of various modifications on lepton anomalies will be found in Bailey and Picasso (1970). We will confine our attention to a general discussion of the various types of proposed modifications and criticisms of QED.

In a generalized sense, our current formulation of QED is based on two specific assumptions. The first assumption has to do with the exact nature of the basic, or lowest-order interaction between a charged particle and the electromagnetic field. With the knowledge that the coupling constant e associated with this interaction is small, we then introduce the second assumption, which is that we can calculate the properties of actual physical systems through the use of perturbation theory expansions in $e^2(\alpha)$. A lack of validity in either of these basic assumptions then leads to a "breakdown" of QED at some level of accuracy.

Speculation as to the nature of modifications to the basic interaction of QED has been both prolific and varied. Modifications fall into three basic categories:

(1) Introduction of a fundamental distance associated with electromagnetic interactions. That is to say, the charge distribution of the lepton may have a finite extent. In this case, the normal undressed form factor $F_{e,\mu}(q^2)=1$ is replaced by a factor

$$F_{e,\mu}(q^2)=\Lambda^2_{e,\mu}/(\Lambda^2_{e,\mu}+q^2).$$

The parameter Λ is specific to each type of lepton. The effect of such a modification on the anomaly is (Berestetskij, *et al.*, 1956)

$$\delta a/a=-\tfrac{2}{3}(m^2/\Lambda^2).$$

For equal accuracy in a, the muon experiments are therefore a factor of 200 times as sensitive in setting limits on Λ, assuming that the deviation between theory and experiment is due to a finite Λ. The most recent muon measurement (with an accuracy of 270 ppm) implies $\Lambda_\mu>7$ GeV, while the most recent electron experiment (3 ppm) implies $\Lambda_e>0.2$ GeV (both values correspond to a 95% confidence level). Colliding electron experiments (Barber, *et al.*, 1966) imply $\Lambda_e>6$ GeV.

(2) *Ad hoc* modifications to the photon or lepton propagators. For instance, in the photon propagator, $1/q^2$ can be replaced by

$$(1/q^2)[\Lambda^2_\gamma/(\Lambda^2_\gamma+q^2)].$$

The shift in a is similar to that given for case (1). Lee and Wick (1969) have considered the implications of such a modification.

Arbitrary modifications of the lepton propagator have a similar effect on a. However, it should be noted that most modifications of the lepton propagator violate the principle of charge conservation (gauge invariance). Kroll (1966) has pointed out that in order to maintain charge conservation, modification of the lepton propagator requires a corresponding modification of the vertex function. With the exception of propagators in closed Fermion loops, these two modifications almost nullify each other, rendering the over-all effect undetectable!

(3) Coupling of leptons to a presently unknown field of mass M, with coupling constant f. The effect of such a field on the anomaly is $\delta a=Cf^2(m/M)^2$, where C is a numerical constant and m is the lepton mass (Bailey and Picasso, 1970). A massive field would have an appreciable effect only at high q^2 (small distances). Such a field could account for the $\mu-e$ mass difference.

At the present time, questions as to whether a perturbation theory approach to QED is valid, and more specifically, whether power series expansions of the type given in Eq. (1.2) converge, remain unanswered. Although mass and charge renormalization insure that the coefficients in such series expansions are finite and, in principle calculable, the fact that α is much less than unity does not insure that the series converges, either absolutely, or even asymptotically. Speculation on the convergence of QED has provided few insights as to the observable consequences of a breakdown of this type. In view of the results of current experiments, QED appears to hold through at least fourth order, and perhaps through sixth order. Thus, any remaining effect is expected to be of a subtle nature. When one considers the expected magnitude of the eighth- and higher-order contributions to the lepton anomalies [$(\alpha/\pi)^4$ is 0.02 ppm of a], it can be seen that straightforward tests of the convergence of QED will place very stringent requirements on the accuracy of future experiments.

In conclusion, it is clear that while some aspects of the present formulation of QED are unsatisfactory from an esthetic viewpoint, in an operational sense the theory is remarkably successful in predicting with great pre-

cision, the properties of diverse quantum systems. Definitive evidence of a breakdown would, of course, be very exciting, as it might lead to a better understanding of presently inexplicable problems such as the $\mu-e$ mass difference. However, until such evidence for failure of the theory is found, modifications of QED must remain in the realm of speculation.

III. CURRENT EXPERIMENTS

At the present time, two distinct experimental techniques have been developed to permit precision measurements of lepton g-factor anomalies. The first technique is that used in the Michigan electron experiments and the CERN muon experiments. The distinguishing feature of these experiments is a direct observation of the spin precession of polarized leptons in a region of static magnetic field. We will refer to these experiments as precession experiments. The second technique is that employed in the experiments at Washington, Mainz, and Stanford. The distinguishing feature of these experiments is the presence of an oscillating electromagnetic field that induces transitions between energy levels of a lepton interacting with a static magnetic field. We will refer to experiments of the second type as resonance experiments.

The division in experimental technique noted above has been accompanied by a corresponding division in the theory used to analyze the respective experiments. The analysis of the precession experiments has been formulated in terms of classical solutions to the equations of motion of a macroscopic particle, while the analysis of the resonance experiments has usually been formulated in terms of quantum-mechanical solutions to the energy eigenvalue problem of an electron in specific combination of electric and magnetic fields. With the exception of the Stanford experiment, the introduction of quantum mechanics is a matter of convenience, rather than necessity. We will begin with a discussion of the precession experiments, and of the classical theory used for their interpretation. We will then consider the resonance experiments, and where possible, point out some of the similarities of two techniques. Finally, we will discuss the relative advantages and difficulties of each experiment of current interest, and conclude with a summary and comparison of current experimental results and theoretical calculations.

3.1 The Precession Method

3.1.1 *General Discussion*

Consider the case of a lepton with velocity $\mathbf{v}$ moving perpendicular to a uniform magnetic field $\mathbf{B}$. The orbital motion of the lepton will be a uniform rotation of $\mathbf{v}$ at the cyclotron frequency[5] $\omega_c=\omega_0/\gamma$, where $\omega_0=eB/mc$, $\gamma=(1-v^2/c^2)^{-1/2}$, and m is the lepton rest mass. The spin motion, as viewed in the laboratory frame, will be a uniform precession of $\mathbf{S}$ at the spin precession frequency $\omega_S=(g/2)\gamma\omega_c+(1-\gamma)\omega_c$. The first term in this expression is the precession frequency one would obtain for a lepton undergoing unaccelerated motion. The second term is the Thomas precession frequency due to the acceleration associated with the lepton's uniform circular motion. The relative precession of $\mathbf{S}$ with respect to $\mathbf{v}$ will occur at a frequency $\omega_S-\omega_c$. Defining this difference or g-2 frequency as ω_D, and inserting the above expressions for ω_S and ω_c, we obtain the surprisingly simple result:

$$\omega_D=a\omega_0. \tag{3.1}$$

Although both ω_S and ω_c depend on γ, their difference is completely independent of velocity. This fortunate circumstance permits measurements of a without corrections for particle energy, at least to lowest order. Consequently, experiments to measure a span a range from $v/c=0.997$ (the CERN muon measurement at 1.3 GeV) to $v/c=10^{-7}$ (the Stanford electron measurement at 10^{-8} eV). In each experiment, the relativistic corrections are negligible!

The total angle of precession of $\mathbf{S}$ with respect to $\mathbf{v}$ from time $t=0$ to $t=T$ will be

$$\theta_D=\omega_D T, \tag{3.2}$$

so that $\hat{S}\cdot\hat{v}$ (a quantity proportional to the lepton helicity) will vary as $\cos\omega_D T$. A device (polarimeter) with an output proportional to $\hat{S}\cdot\hat{n}$ ($\hat{n}$ defines a fixed direction in space) can be used to measure ω_D by means of the scheme shown in Fig. 3.1. Assume that we prepare a polarized[6] lepton beam and then inject it into a cyclotron orbit perpendicular to a region of uniform magnetic field $\mathbf{B}$. At time $t=T$, we measure $\hat{S}\cdot\hat{v}$ with the polarimeter. If this experiment is repeated for various values of T, the polarimeter output will vary as $\cos\omega_D T$, so that if N complete oscillations of the output are observed between $T=T_1$ and $T=T_2$, then

$$\omega_D=2\pi N/(T_2-T_1). \tag{3.3}$$

The accuracy to which ω_D can be determined will increase in direct proportion to N, all other factors being equal, so that the most obvious way to improve the precision of the measurement is to increase the time the particle spends in the magnetic field. In a precision experiment, N is typically of the order of 10^3. Since $a\cong 10^{-3}$, this implies about 10^6 cyclotron revolutions

---

[5] All references to frequency in this article are to angular frequency (radians/sec) unless otherwise noted. We reserve the notation ω for angular frequency, and the notation $f=\omega/2\pi$ (in Hz) for circular frequency.

[6] We define polarization ($\mathbf{P}$) in the usual manner; i.e., $\mathbf{P}=\langle\hat{S}\rangle$, where the brackets indicate an ensemble average. All references to $\mathbf{S}$ or $\hat{S}$ are to be understood in terms of $\mathbf{P}$.

from injection to analysis. If only a uniform magnetic field is used, any component of $\mathbf{v}$ parallel to $\mathbf{B}$ will cause the orbit to drift parallel to the field direction. Since all practical lepton sources have a finite angular emittance, it is not possible to confine a useful number of leptons for the desired periods using only a uniform magnetic field.[7] Some sort of axial focusing scheme is required. The usual choice has been magnetic focusing, in the form of a magnetic-mirror trap, or a weak-focusing storage ring. Although either of these schemes permits greatly increased storage times, the increase is obtained at the expense of perturbations to the difference frequency precession introduced by the focusing fields. In precision experiments, the effects of these perturbations must be considered carefully.

In addition to the magnetic field in the storage region, weak electric fields may also be present. These stray fields may be due to contact potential variations between metallic surfaces enclosing the storage region, charging of dielectric surface films, or space charge of the trapped beam. Although these fields are quite weak, (typically $E/B<10^{-4}$), they can result in significant additional perturbations to the difference frequency.

The generalized problem can be stated as follows: The fields in the storage region will consist of a nearly homogeneous magnetic field $\mathbf{B}(\mathbf{r})$, as well as a weak, but not necessarily homogeneous electric field $\mathbf{E}(\mathbf{r})$. Given initial conditions for $\mathbf{S}$ and $\mathbf{v}$, we wish to solve for the resultant motion of $\mathbf{S}(t)$ and $\mathbf{v}(t)$ in the fields $\mathbf{B}(\mathbf{r})$ and $\mathbf{E}(\mathbf{r})$. The rate of variation of $\hat{S}(t)\cdot\hat{v}(t)$ can then be identified as ω_D, as obtained from Eq. (3.3).

The problem of computing the spin precession of a particle in general electric and magnetic fields has been considered by Bargmann, Michel, and Telegdi (1959), Ford and Hirt (1961), and Fierz and Telegdi (1970), and reviewed by Farago (1965). Although the formulations are equivalent, we find the most explicit to be that of Ford and Hirt. They have shown that the exact[8] classical relativistic equations of motion of a particle with spin $\mathbf{S}$, magnetic moment $(g/2)(e/mc)\mathbf{S}$, and electric dipole moment[9] $(f/2)(e/mc)\mathbf{S}$ in laboratory fields

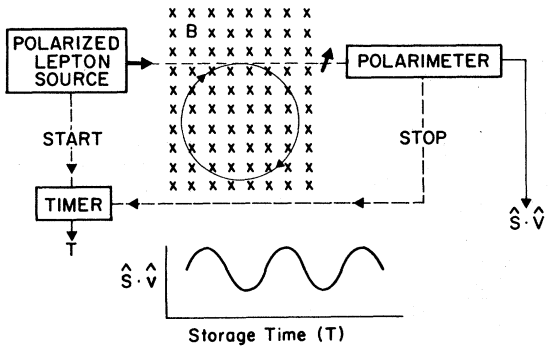

FIG. 3.1. Schematic outline of the precession experiments.

$\mathbf{B}(\mathbf{r})$ and $\mathbf{E}(\mathbf{r})$ can be put into the form:

$$d\hat{v}/dt=\boldsymbol{\Omega}_v\times\hat{v}, \tag{3.4}$$

$$d\mathbf{S}/dt=\boldsymbol{\Omega}_S\times\mathbf{S}, \tag{3.5}$$

where

$$\boldsymbol{\Omega}_v=-(e/mc)\{\mathbf{B}/\gamma-[\gamma/(\gamma^2-1)]\boldsymbol{\beta}\times\mathbf{E}\},$$

$$\begin{aligned}\boldsymbol{\Omega}_S=-(e/mc)\{&(\mathbf{B}/\gamma)-(\gamma/(\gamma+1))\boldsymbol{\beta}\times\mathbf{E}\\&+a[\mathbf{B}-(\gamma/(\gamma+1))\boldsymbol{\beta}(\boldsymbol{\beta}\cdot\boldsymbol{\beta})-\boldsymbol{\beta}\times\mathbf{E}]\\&+\tfrac{1}{2}f[\mathbf{E}-(\gamma/(\gamma+1))\boldsymbol{\beta}(\boldsymbol{\beta}\cdot\mathbf{E})+\boldsymbol{\beta}\times\mathbf{B}]\},\end{aligned}$$

and $\boldsymbol{\beta}=\mathbf{v}/c$. The vectors $\boldsymbol{\Omega}_v$ and $\boldsymbol{\Omega}_S$ are analogous to ω_c and ω_S for the case of planar cyclotron motion. Although $\boldsymbol{\Omega}_v$ and $\boldsymbol{\Omega}_S$ will not, in general, be parallel, it is still possible to define a difference frequency vector $\boldsymbol{\Omega}_D$, analogous to ω_D, as

$$\begin{aligned}\boldsymbol{\Omega}_D=\boldsymbol{\Omega}_S-\boldsymbol{\Omega}_v=-(e/mc)\{&a\mathbf{B}-a(\gamma/(\gamma+1))\boldsymbol{\beta}(\boldsymbol{\beta}\cdot\mathbf{B})\\&+((1/\beta^2\gamma^2)-a)\boldsymbol{\beta}\times\mathbf{E}\\&+\tfrac{1}{2}f[\mathbf{E}-(\gamma/(\gamma+1))\boldsymbol{\beta}(\boldsymbol{\beta}\cdot\mathbf{E})+\boldsymbol{\beta}\times\mathbf{B}]\}.\end{aligned} \tag{3.6}$$

The equation of motion of $\mathbf{S}$ in the electron rest frame is simply

$$d\mathbf{S}/dt=\boldsymbol{\Omega}_D(\mathbf{v},\mathbf{B},\mathbf{E})\times\mathbf{S}. \tag{3.7}$$

The instantaneous motion of $\mathbf{S}$ with respect to $\mathbf{v}$ will be a precession of $\mathbf{S}$ about $\boldsymbol{\Omega}_D$ with angular velocity $\omega_D=|\boldsymbol{\Omega}_D|$ (Fig. 3.2).

In practice, a solution for $v(t)$ sufficiently accurate for the experiments under consideration can be obtained without an exact integration of Eq. (3.4). Depending on the particular experiment, such a solution follows from the use of the adiabatic invariance of the orbital magnetic moment,[10] linearized equations of motion, or numerical integration. This solution can then be inserted into Eqs. (3.6) and (3.7), and a solu-

[7] Consider a particle injected with a small pitch angle α with respect to the plane normal to $\mathbf{B}$. Then we have $v_z\cong v\alpha$, and $z\cong 2\pi r_c\, n\alpha$, where n is the number of cyclotron orbits, r_c is the cyclotron radius, and z is the axial drift distance. For $\alpha=10^{-2}$, $r_c=10$ cm, and $n=10^6$, we find $z=6000$ m! A single pass through a long solenoid is therefore ruled out, at least in terms of a practical experiment.

[8] The instantaneous fields experienced by the particle are assumed to be homogeneous, in the sense that forces of the type $\nabla(\boldsymbol{\mu}\cdot\mathbf{B})$ are negligible compared to the Lorentz force in these experiments, and are therefore not included in the equations of motion for $\mathbf{v}$ or $\mathbf{S}$.

[9] Although symmetry considerations require the edm of a Dirac particle to be identically zero, a possible finite edm is included for completeness. The current upper limit on the electron edm is 2×10^{-21} e cm (Sandars and Lipworth, Phys. Rev. Letters **13**, 718 1964), corresponding to $f<1.8\times10^{-10}$. The effect of the electron edm will be completely negligible at the level of 1 ppm in a. Accordingly, the terms proportional to f can be dropped from Eq. (3.6).

[10] The orbital moment is defined as IA/c, where $I=e\omega_c/2\pi$ is the current due to the circulating lepton, and $A=\pi r_c^2$ is the area of the orbit. For a uniform field B, we have $\mu_{\rm orb}=T_\perp/B$, where $T_\perp=\frac{1}{2}\gamma m v_\perp^2$, and $v_\perp$ is the component of $\mathbf{v}$ perpendicular to $\mathbf{B}$.

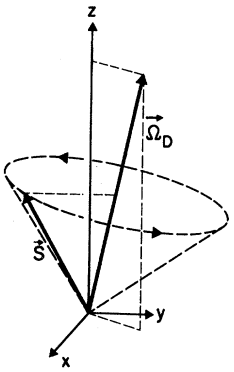

FIG. 3.2. Precession of the spin vector about the difference frequency vector in the electron rest frame.

tion for $\mathbf{S}(t)$ could conceivably be obtained by further integration. In practice, such an approach is not feasible except for certain simple cases, such as helical motion in a uniform magnetic field. Fortunately, a satisfactory solution to the problem can be obtained by employing certain approximations that are based on the following properties of the orbital motion and fields in the precession region: (a) $\mathbf{v}(t)$ can be separated into two essentially decoupled motions, consisting of (1) cyclotron motion at frequency ω_c, and (2) an axial oscillation at frequency ω_z; (b) ω_D is small in comparison to ω_c, and is in general not commensurate with ω_z; and (c) the variation of $\mathbf{E}(\mathbf{r})$ and $\mathbf{B}(\mathbf{r})$ over the storage region is small compared to the magnitude of $\mathbf{B}$. Accordingly, perturbation methods can be employed to calculate the average motion of $\mathbf{S}$. These calculations show that, neglecting correction terms of order v_z^2/c^2, the spin motion observed in the precession experiments is a uniform precession about the direction $[\boldsymbol{\Omega}_D]$ at a frequency $[\omega_D]=[|\,\boldsymbol{\Omega}_D\,|]$ (v_z is the axial component of $\mathbf{v}$; see Sec. 3.1.2 for a more complete discussion of the correction terms). In the above, the notation [ ] indicates that the enclosed quantity is to be time-averaged over a complete period of $\mathbf{v}(t)$. Although the fields in the storage region are static, the electrons experience a time-varying field due to their orbital and axial motion. The time-average value of the fields "seen" by an electron can be calculated by combining measurements of $\mathbf{E}(\mathbf{r})$ and $\mathbf{B}(\mathbf{r})$ with knowledge of $\mathbf{v}(t)$.

In addition to measuring ω_D, it is also necessary to measure or obtain ω_0. This is usually done indirectly by measuring the magnetic field in the storage region with NMR techniques. The proton resonance frequency can be converted to an equivalent zero-energy cyclotron frequency by the use of accurately measured atomic constants. We will discuss the conversion further in the sections devoted to individual experiments.

3.1.2 *The Michigan Electron Experiments*

The method employed in the Michigan g-2 experiments for the measurement of ω_D is shown in schematic form in Fig. 3.3. The entire experiment takes place in a region of nearly uniform magnetic field. The field at either end of the storage region is slightly stronger than that in the center, and thus forms a magnetic mirror trap. Mott scattering (elastic nuclear Coulomb scattering of electrons in the energy range 1 KeV–1 MeV) is used to polarize the electrons and to analyze their final spin orientation.

The apparatus operates in a cyclic manner. One complete cycle (the unit experiment) consists of the following sequence of events: a pulse of 100 KeV electrons moving parallel to $\mathbf{B}$ is scattered from the polarizing foil. Those electrons which scatter nearly perpendicular to the magnetic field are transversely polarized ($\hat{S}\cdot\hat{v}=0$) with $\mathbf{S}$ perpendicular to the magnetic field. The degree of polarization is approximately 20%. These electrons spiral into the trapping region, which is enclosed by a pair of cylindrical electrodes. As the electrons drift across the gap between the cylinders, a momentary voltage applied to the injection cylinder causes them to lose sufficient axial velocity so that they become permanently trapped in the magnetic field. The electrons oscillate back and forth in the trap for a predetermined time T, until a second momentary voltage pulse applied to the ejection cylinder gives them sufficient axial velocity to reach the analyzing foil. Here they undergo a second Mott scattering. Those which scatter parallel to the magnetic field are counted. The probability of scattering parallel to z is proportional to $\hat{S}\cdot(\hat{v}\times\hat{z})$. Because of the g-2 precession, the number of electrons scattered into the detector as a function of T (assuming that the number of electrons ejected from the trap is independent of T) will be

$$R(T)=R_0\{1+\delta\cos(\omega_D T+\phi)\}. \qquad (3.8)$$

Here δ is the Mott asymmetry factor (typically 0.01–0.05), and ϕ is a phase constant. The difference frequency is determined by sampling $R(T)$ as a function of T at two widely separated values of trapping time. By fitting the data of $R(T)$ vs. T, the position of two maxima of $R(T)$ can be established to be at $T=T_1$ and $T=T_2$. By taking a nominal amount of additional data between the two selected maxima, N can be established without an explicit counting of all of the intermediate cycles. Equation (3.3) can then be used to calculate ω_D.

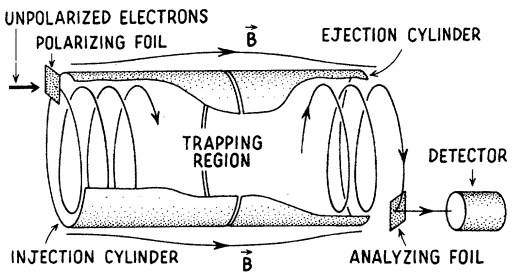

FIG. 3.3. The Michigan electron g-2 experiments.

For electrons in a magnetic trap in the presence of a radial electric field E_r, with $\gamma^2 \ll a^{-1}$,[11] and for $\omega_D \gg \omega_z$ (ω_z is the axial oscillation frequency—Sec. 3.1.1), the observed difference frequency $\langle[\omega_D]\rangle$ will be given by

$$\langle[\omega_D]\rangle/\langle[\omega_0]\rangle = a - a(\langle[v_z^2]\rangle/2c^2) - (\langle[E_r]\rangle/\beta\gamma^2 B), \tag{3.9}$$

where the notation $\langle\ \rangle$ indicates that the enclosed quantity is to be averaged over the ensemble of electrons in the trap.[12] The quantity $\langle[\omega_D]\rangle$ is the average frequency obtained from the trapping time difference between maxima of $R(T)$, i.e., it is measured directly. The quantities $[\omega_0]$ and $[v_z^2]$ can be calculated by combining knowledge of the axial motion with measurements of the axial dependence of the magnetic field. The axial motion can itself be obtained from measurements of the axial field dependence, coupled with use of the adiabatic invariance of the orbital magnetic moment. Once the time-average quantities are calculated as a function of the axial oscillation amplitude, the ensemble averages can be evaluated from direct measurements of the amplitude distribution of the trapped electrons. The magnetic field is measured in terms of the NMR frequency $\omega_p(H_2O)$ of protons in a water sample. This frequency can be converted to $\omega_0(e^-)$ using the relation

$$\omega_0(e^-) = \omega_p(H_2O)\,(\mu_p'/\mu_B)^{-1} \tag{3.10}$$

The ratio μ_p'/μ_B, (the magnetic moment of the proton in Bohr magnetons, uncorrected for diamagnetism) is known to better than 0.1 ppm (Taylor, Parker, and Langenberg, 1969).

We have now arrived at a major point of difficulty associated with the Michigan work (similar problems are present in other electron g-2 experiments, as we will discuss later). This difficulty is the presence of the $\langle[E_r]\rangle$ term in Eq. (3.9). The shift in ω_D due to this term cannot be ignored. The *time-average* radial field encountered in the trapping region is typically about 1 mV/cm. For the range of magnetic fields used in the most recent Michigan experiment, the corresponding relative shift in $\langle[\omega_D]\rangle$ is of order 3–10 ppm. The radial fields in the trapping region that contribute to $[E_r]$ are estimated to be of order 10–100 mV/cm.[13] Such fields are too small to be directly measured, especially under operating conditions. Consequently, one must resort to an extrapolation procedure to determine the effect of the electric field. Equation (3.9) can be rearranged into the form

$$a' = \langle[\omega_D]\rangle/\langle[\omega_0]\rangle\{1+(\langle[v_z^2]\rangle/2c^2)\}, \tag{3.11}$$

where all quantities on the right-hand side are experimentally measurable or calculable, and where

$$a' \equiv a - \{\langle[E_r]\rangle/\beta\gamma^2 B\} = a - \langle[E_r]\rangle X$$

is the apparent value of the anomaly, shifted from the true anomaly by an amount $\langle[E_r]\rangle X$. If $\langle[E_r]\rangle$ is independent of X, a can be obtained by measuring $a'(X)$ at several values of X and extrapolating the results to $X=0$.

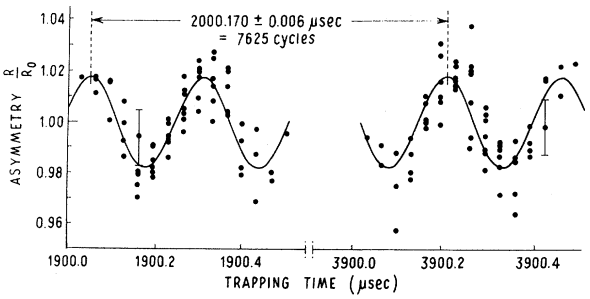

FIG. 3.4. Typical data from the recent Michigan electron experiment.

Figure 3.4 shows a typical data run from the most recent Michigan experiment. The statistical accuracy in determining the position of the maxima is sufficient to determine $\langle[\omega_D]\rangle$ to 3 ppm in a single data run (about 24 hours). The magnetic field used in this experiment is shown in Fig. 3.5, and the measured values of a' vs X in Fig. 3.6. The linear extrapolation shown corresponds to a radial electric field of (0.4 ± 0.6) mV/cm.

Table I summarizes some of the parameters and the results of the Michigan experiments.

3.1.3 *The Michigan Positron Experiments*

The Michigan g-2 technique has been extended to measurements of the positron anomaly by Rich and Crane (1966) and Gilleland and Rich (1969). The

[11] Note that in Eq. (3.6), the coefficient of the $\boldsymbol{\beta}\times\mathbf{E}$ term is $\beta^{-2}\gamma^{-2}-a$. For $\beta\cong1$ and $\gamma\cong1$, the effect of the anomaly can be neglected. See Sec. 4.3 for a further discussion of this point.

[12] S. Granger and G. W. Ford have recently obtained a perturbation solution of the general spin motion problem for an electron in a weak magnetic mirror trap. Their preliminary results show that if $\omega_D \ll \omega_z$, Eq. 3.9 should be written as:

$$\langle[\omega_D]\rangle/\langle[\omega_0]\rangle = a - \tfrac{1}{2}a(\langle[v_z^2]\rangle/v^2) - (\langle[E_r]\rangle/\beta\gamma^2 B),$$

where v the total speed of the electron replaces the "c" of Eq. (3.9). If $\omega_D \gg \omega_z$, Eq. 3.9 is correct. The condition $\omega_D \ll \omega_z$ characterizes the Wilkinson–Crane experiment. A recalculation of the WC data as revised by Rich (Rich, 1968), but based on the new equation for $[\omega_D]$ shows that the result for "a" should be increased by about five standard deviations. It is now about one standard deviation higher than the latest experimental measurement and the theoretical value. This lays to rest the heretofore puzzling 3.5 standard deviation discrepancy between the revised WC result and the more recent work, (Wesley–Rich, 1971; Levine–Wright, 1971). In the current electron g-2 experiment (WR, 1971) we find $\omega_D \simeq 3\omega_z$ and an exact evaluation shows that a correction of less than one standard deviation must be made. This correction slightly improves the agreement between experiment and theory. Details of the above calcaultion have been submitted for publication by Granger and Ford.

[13] Since there are no field sources (except for space charge, which is negligible) located within the trapped beam, the oscillatory motion of the electrons results in a great deal of cancellation in $[E_r]$. A factor of ten reduction is typical.

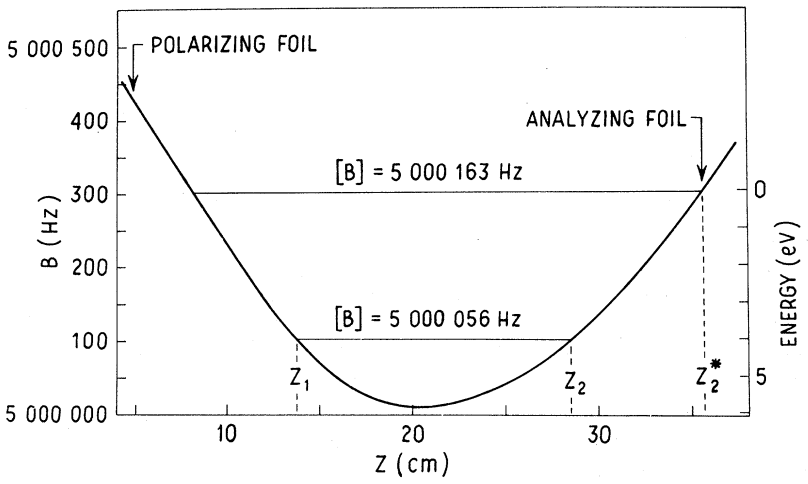

FIG. 3.5. Magnetic field profile of the Michigan g-2 Experiment.

method employed is similar to that used for the electron experiments except for the means used to polarize and analyze the positrons.

The positrons used in the measurement are obtained from a Co^{58} source. Because of parity nonconservation in beta decay, the positrons are longitudinally polarized, with polarization equal to v/c, about 0.7 in the Michigan work. An annular collimator permits those positrons with the desired momentum and orbit centers to enter the trapping region. Considerations such as cost and shielding limit the maximum source strength to about 1 Curie (Ci) of Co^{58} (15% positron decay ratio). For a source of this strength, the average number of positrons trapped per machine cycle is about 10^{-3}, some seven orders of magnitude less than the corresponding number in the electron experiments. This extremely low trapping rate rules out the use of Mott scattering for the analysis of the ejected positrons.[14]

Fortunately, a more efficient method is available, in the form of a positron polarimeter, first suggested by Telegdi.[15] The device is based on the formation and subsequent decay of positronium in a strong magnetic field. The over-all efficiency of the polarimeter is about 0.1, i.e., 10% of the incident positrons yield useful information on the polarization of the incoming beam. The corresponding efficiency of Mott scattering is about 10^{-4}. The increased efficiency of the positronium polarimeter is instrumental in making the positron experiment practical.

The polarimeter consists of a plastic scintillator immersed in a magnetic field $\mathbf{B}_p$ ($\mathbf{B}_p \cong 10$ kG) and a delayed coincidence system for detecting the annihilation radiation of positronium formed by positrons stopped in the scintillator (Fig. 3.7). The ejection is arranged so that the positrons ejected from the trapping field enter the polarimeter with their velocity $\mathbf{v}$ parallel to $\mathbf{B}_p$. Furthermore, during the ejection process $\hat{S}\cdot\hat{v}$ is conserved (except for a small g-2 rotation), so $\hat{S}\cdot\hat{B}_p$ will vary as $\hat{S}\cdot\hat{v}$. Approximately half of the positrons stopped in the scintillator form positronium. The relative ratios of the amounts of the field-perturbed $m=0$ singlet and triplet states of positronium will vary as $\hat{S}\cdot\hat{B}_p$, and hence as $\hat{S}\cdot\hat{v}$. Since the field-perturbed singlet lifetime is much shorter than the field-perturbed triplet lifetime, the number of coincidences observed in a time interval delayed several singlet lifetimes from the positron arrival will exhibit an asymmetry proportional to $\hat{S}\cdot\hat{v}$.[16] For the parameters and coincidence circuitry used in the Michigan experiments, the observed asymmetry was about 2%, that is, equivalent to $\delta=0.02$ in Eq. (3.8).[17]

The principal difficulties in the positron experiment arise from the relatively small intensity of useful positrons that can be obtained from the radioactive source. In order to increase the data collection rate,

[14] If Mott scattering were used, a single data run would require over 10 years. It is interesting to note that in the electron experiments, the beam intensity after the first Mott scattering is equivalent to a 10^8 Ci polarized electron source.

[15] See L. Grodzins, [Progr. Nucl. Phys. **7**, 219 (1959)]. The first demonstration of the effect was by L. Dick, L. Feuvrais, and V. L. Telegdi, "Aix En Provence Intern. Conf. on Elem. Particles", (1961), Vol. VI, 295.

[16] An exact analysis of the $\mathbf{S}\cdot\mathbf{B}$ asymmetry may be found in: A. Rich and H. R. Crane, Proceedings International Conference on Positron Annihilation, (Academic, New York, 1967), p. 321; and in A. Rich, Ph.D. thesis, University of Michigan, 1965 (unpublished). A more intuitive argument for the existence of the effect can be made as follows: In the high field limit ($\mu_e B \gg$ positronium hfs), the $m=0$ triplet state goes to $\downarrow\uparrow$, while the $m=0$ singlet state goes to $\uparrow\downarrow$ (first arrow e^+, second arrow e^-, quantized along $\mathbf{B}_p$). Spin-up positrons will therefore form only singlet positronium, and spin-down positrons will form only triplet positronium. The lifetime difference between these two states would then lead to a decay asymmetry. This high field analysis ignores the fact that the perturbed singlet and triplet lifetimes become equal in the limit of infinite field. Therefore, the asymmetry does not increase with increasing B_p. The optimum value of B_p is about 13 kG for the Michigan experiments.

[17] For a "perfect" coincidence circuit (one with a time resolution much less than the singlet lifetime) the calculated asymmetry is about 6%. The finite time resolution degrades the actual asymmetry to 2%.

TABLE I. Michigan g-2 experiments.

Reference	Particle	Energy (KeV)	Magnetic field (G)	Trap depth (ppm)	Extrapolation (ppm)	Accuracy (ppm)	Result
Schupp, Pidd, and Crane (1961)	e^-	50–100	82–117	2 500	7000	2100	0.0011609(24)
Wilkinson and Crane (1963)	e^-	45–114	94–153	400	40	24	0.001159622(27)
Rich (1968)[a]	...	...	...	...	70	27	0.001159549(30)[a]
Rich and Crane (1966)	e^+	210[b]	220[b]	20 000	...[b]	4800	0.0011680(55)
Gilleland and Rich (1969)	e^+	270[b]	260[b]	3 000	...[b]	1000	0.0011603(12)
Wesley and Rich (1971)	e^-	56–108	820–1170	40	2	3	0.0011596577(35)

[a] The revised Wilkinson–Crane value is the result of the reanalysis of the original data by Rich. See this reference for further comments.

[b] In the positron experiments, only a single combination of magnetic field and particle energy was employed. Consequently, no electric field extrapolation was possible.

the relative depth of the magnetic trap employed in the positron experiments was substantially greater than that used in the electron experiments (see Table I). The low counting rate also made it impractical to measure a' at several values of X. Consequently, no electric field extrapolation was possible. However, on the basis of the electric fields encountered in Michigan electron experiments of similar geometry, the electric field correction in the positron experiments is estimated to be small compared to the final statistical uncertainty in ω_D. Statistical uncertainty contributes approximately 90% of the final error of 950 ppm.

3.1.4 *The Edinburgh Electron Experiment*

An experiment of Farago, Gardiner, Muir, and Rae (1963) performed at the University of Edinburgh employs an interesting variation of the precession technique. The essential distinction between this experiment and the Michigan experiments lies in the method for storing electrons. In the Edinburgh experiment, a weak electric field **E** is superimposed perpendicular to an essentially[18] uniform magnetic field **B** (Fig. 3.8). The orbital motion of polarized electrons emitted from an S^{35} beta source consists of uniform planar cyclotron motion, plus a slow drift of the orbit center in the direction $\mathbf{E}\times\mathbf{B}$. Mott scattering is used to analyze the final spin orientation of the electrons. The number of cyclotron orbits between the source and the analyzing foil (n) can be controlled by varying the magnitude of **E**. Because of the g-2 precession, the counting rate for electrons scattered from the second foil will be

$$R=R_0[1+\delta\sin(2\pi n/n_0)], \qquad (3.12)$$

where R_0 is the rate for an unpolarized beam, and $n_0=(a\gamma)^{-1}$ is the number of orbits required for a single g-2 rotation. Figure 3.9 shows the experimental results of the normalized counting rate plotted as a function of n, where n is calculated from knowledge of the distance between the source and analyzing foil and the strength of E and B. A least-squares fit to the data, combined with measurements of the magnetic field, yields $a_{e^-}=0.001153(23)$.

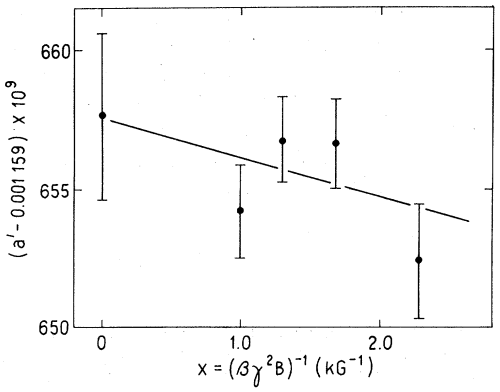

FIG. 3.6. Michigan magnetic field extrapolation.

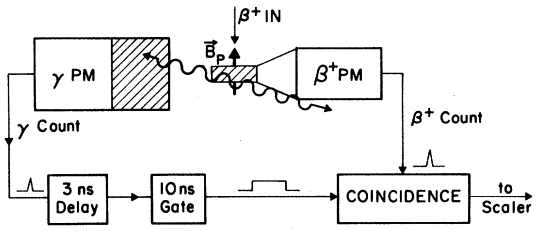

FIG. 3.7. Outline of the Michigan g-2 positron polarimeter.

[18] Slight inhomogeneities are introduced to provide vertical focusing of the electrons.

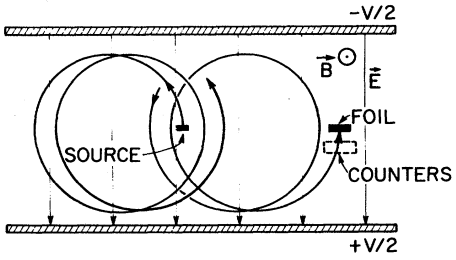

FIG. 3.8. Schematic diagram of the Edinburgh electron experiment.

The principal advantage of an experiment of this type is that it is conducted on a dc (continuous) basis, rather than on a cyclic basis, as in the Michigan experiments. The data rates are therefore considerably higher. On the other hand, less than a single g-2 rotation was employed. An attempt to significantly increase the number of g-2 rotations by reducing the magnitude of **E** leads to defocusing of the electron beam by residual imperfections in the magnetic field. Consequently, the accuracy of this method appears to be limited to about 1% of the anomaly.

3.1.5 *The CERN Muon Experiments*

The current CERN muon experiments are based on confinement of high-energy muons in a weak-focusing storage ring. The apparatus is shown in Fig. 3.10. The storage ring is in the form of a circular iron C magnet, with a field of 17 kG and a mean radius of 2.5 meters, corresponding to a muon momentum of 1.28 GeV/c. The field in the orbital region varies as a function of the orbital radius r in a manner such that the field index n, $[n=(r/B)\partial B/\partial r]$, is approximately 0.13. This field configuration results in focusing in both the radial and vertical directions.

Polarized muons are produced and injected into the ring in the following manner: A pulse of 10.5 GeV/c protons from the CERN proton synchrotron is allowed to strike an internal target within the storage ring, thereby producing a burst of pions and other particles. The pions decay rapidly (with a half-life corresponding to five turns in the ring) to muons and neutrinos

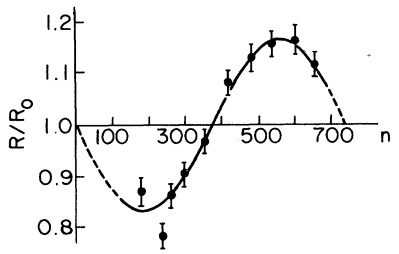

FIG. 3.9. Data from the Edinburgh experiment.

($\pi^{\pm}\rightarrow\mu^{\pm}+\nu_{\mu}$). Either μ^+ or μ^- can be injected, depending on the field polarity selected. Decay muons with momenta in the range (1.28±0.02) GeV/c have the proper injection angle and orbit radius to remain permanently trapped in the ring. While the muons are stored, their lifetime in the lab frame increases by the time dilation factor γ ($\gamma\cong 12$) over the rest lifetime of 2.2 μsec.

Useful numbers of muons remain in the storage ring up to $T=200$ μsec. Since ω_D is independent of γ (Sec. 3.1.1), the total number of g-2 precessions that can be observed is increased by a factor of γ. This increases the over-all accuracy of the experiment by a factor of $\gamma^{1/2}$, about 3.5 in the current work.[19] Somewhat surprisingly, the use of highly relativistic muons provides a very substantial increase in accuracy. Ideally, one would

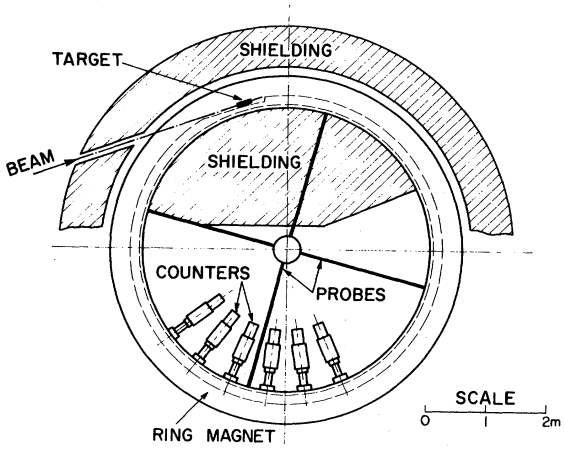

FIG. 3.10. The CERN muon storage ring.

like to use as high an energy as possible (but see Sec. 4.3).

The injection scheme just described favors the trapping of muons that arise from forward decays in the pion rest frame. Since these muons are polarized along the direction of emission (owing to parity nonconservation in weak interactions), the stored muons are partially polarized in the longitudinal direction ($P\cong 0.26$). The muons eventually decay, primarily by the reactions $\mu^+\rightarrow e^+ + \nu_e + \bar{\nu}_{\mu}$; $\mu^-\rightarrow e^- + \bar{\nu}_e + \mu_{\mu}$. In this process, the decay electrons are emitted preferentially parallel to the muon spin. For example, in the muon rest frame, the angular distribution of the decay electrons is given by

$$\frac{Q(\theta)}{d\Omega/4\pi} = 1+\frac{P}{3}(\hat{S}_{\mu}\cdot\hat{v}_e)\equiv 1+P/3\cos\theta. \quad (3.13)$$

[19] All other factors being equal, the error in ω_D is proportional to $N^{-1}N_{2\pi}^{-1/2}$, where N is the number of cycles, and $N_{2\pi}$ is the total number of data counts recorded over one cycle of the difference frequency curve. Since $N\propto\gamma$, while $N_{2\pi}\propto\gamma^{-1}$, the net gain in accuracy is proportional to $\gamma^{1/2}$.

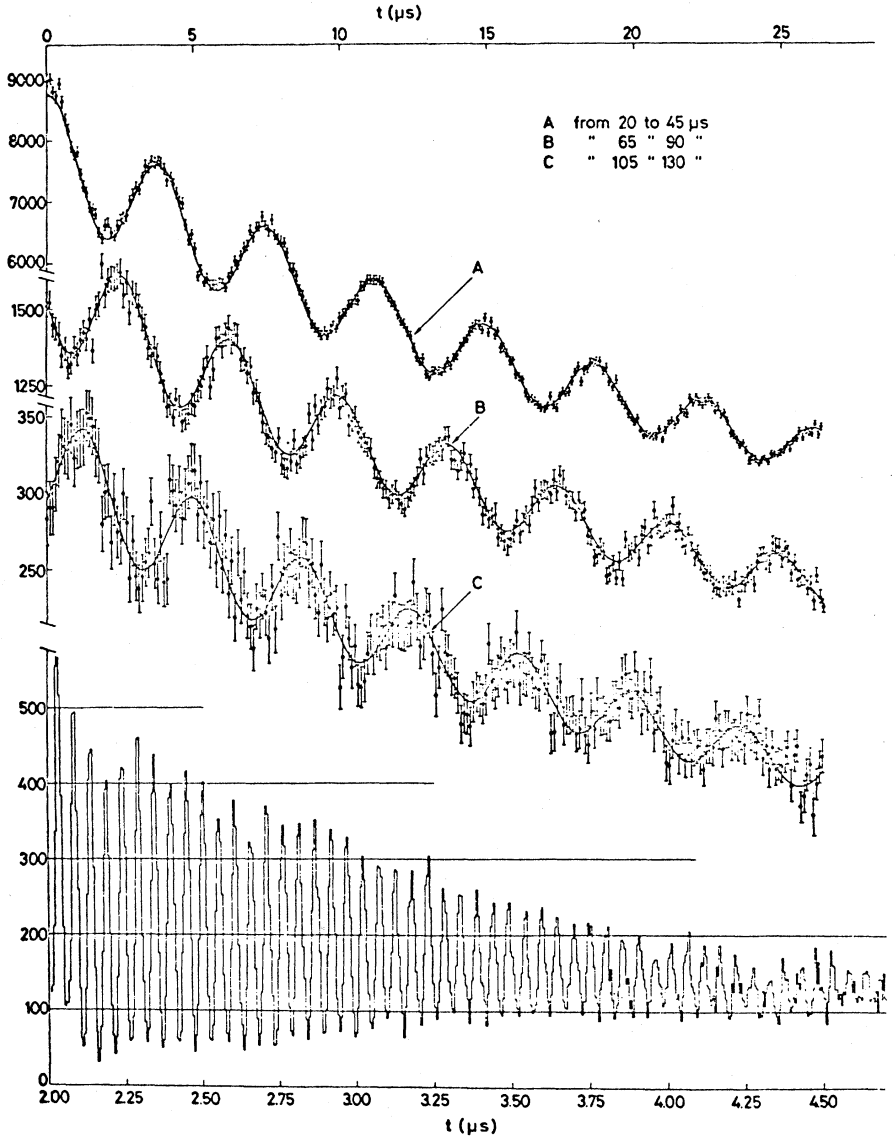

FIG. 3.11. Data from the CERN muon experiment.

Here S_μ is the muon spin, v_e is the electron velocity, P is the muon polarization, and Q is the probability of obtaining a decay electron in the solid angle $d\Omega$. This asymmetry (again due to parity nonconservation) provides the means used to observe the muon g-2 precession.

Because of the combined effects of the g-2 precession of $\mathbf{S}_\mu$ with respect to $\mathbf{v}_\mu$ (the muon velocity) and the $\mu-e$ decay asymmetry noted above, the number of electrons emitted parallel to $\mathbf{v}_\mu$ will vary as $1+A\cos\omega_D t$, where A is an asymmetry parameter. These electrons can be identified in the laboratory frame by their energy. The kinematics of the $\mu-e$ decay provides a correlation between the angle between $\mathbf{v}_\mu$ and $\mathbf{v}_e$, and the electron energy in the lab frame (forward decays tend to have higher energies than backward decays). If we arrange to count only those electrons with an energy E greater than a given value E_c, these electrons must be from forward decays that occur in a cone about $\mathbf{v}_\mu$. Consequently, the number of electrons counted will be modulated at the g-2 frequency, viz:

$$N(E>E_c) \propto 1+A(E_c)\cos\omega_D T.$$

The magnitude of the amplitude A depends on the value chosen for E_c, since this in turn determines the half-angle of the velocity cone of the accepted electrons. The maximum electron energy $E_{\max}$ observed in the labora-

tory frame corresponds to a 45 MeV electron emitted parallel to $\mathbf{v}_\mu$ (for the CERN experiment, $E_{\max}=1300$ MeV). As the cutoff energy E_c approaches $E_{\max}$, A/P approaches unity. Simultaneously, the number of electrons in the allowed momentum band approaches zero. For lower values of the cutoff energy, the number of electrons counted increases, but A/P decreases. In order to collect data in the most efficient manner, one wishes to select a value for E_c that minimizes the uncertainty in ω_D for a given running time.[20] In the CERN experiment, $E_c=780$ MeV, $A/P=0.42$ and $A=0.11$ were found to be optimum. The exact value of E_c is not critical.

If losses from the storage ring due to orbit perturbations are ignored, the expected counting rate as a function of the storage time T will be

$$R(T)=R_0\exp(-T/\tau)\{1+A\cos(\omega_D T+\phi)\}, \quad (3.14)$$

where τ is the laboratory muon lifetime. Figure 3.11 shows the data of the most recent experiment. Unlike the electron experiments, asymmetry data is obtained over a continuous range of T.

Initial attempts to fit the asymmetry data of Fig. 3.11 revealed a significant dependence of ω_D and τ on the particular portion of the data chosen. This difficulty was found to be due to the presence of a residual uniform background and muon losses caused by orbit perturbations. An eight-parameter fit of the form

$$R(T)=R_0\exp(-T/\tau)\{1+A\cos(\omega_D T+\phi)\}\times\{1+R_1\exp(-T/\tau_1)\}+R_2 \quad (3.15)$$

takes these factors into account, and was found to give values of ω_D that showed no statistically significant dependence on the portion of the data used in the least-squares fit.

In addition to ω_D, it is necessary to determine $\omega_0(\mu)$. As in the electron experiments, the magnetic field is measured in terms of $\omega_p(H_2O)$. The conversion constant analogous to μ_p'/μ_B (as used in the electron experiments) is $\lambda\equiv\omega_{\mu^+}(H_2O)/\omega_p(H_2O)$, i.e., λ is the experimentally measured ratio of the precession frequencies of protons and stopped muons, as measured in a water sample. Because of diamagnetic shielding the precession frequency of μ^+ in water will be given by $\omega_{\mu^+}(H_2O)=(1-\epsilon)\omega_{\mu^+}$. Thus we have

$$\omega_{\mu^+}/\omega_p(H_2O)=\lambda(1-\epsilon)^{-1},$$

and since $\omega_{\mu^+}=(1+a_\mu)\omega_0(\mu)$, we obtain

$$\omega_0(\mu)=\lambda(1-\epsilon)^{-1}(1+a_\mu)^{-1}\omega_p(H_2O). \quad (3.16)$$

Ruderman (1966) has calculated the diamagnetic shielding coefficient ϵ to be $\epsilon=(10\pm5)\times10^{-6}$. The quantity λ has been measured by Hutchinson *et al.* (1970) to an accuracy of 9 ppm. These factors introduce negligible uncertainty in the final result for a_μ, since they are considerably smaller than the uncertainties in ω_D and $\omega_p(H_2O)$.

The frequency obtained from fitting the asymmetry data to Eq. (3.15) is actually $\langle[\omega_D]\rangle$, where, for the muon experiments, the time average $[\ ]$ reduces to an azimuthal average over the storage ring, and the ensemble average $\langle\ \rangle$ requires the evaluation of the average radius of the stored muons. During the course of the experiment, the magnetic field is surveyed as a function of both radius and azimuth. The weak-focusing gradient results in a 2000 ppm variation of the magnetic field over the useful aperture of the ring. Since

$$\Delta B/B=n(\Delta\rho/\rho),$$

and since $n=0.13$, a knowledge of the average radius $\langle\rho\rangle$ to an accuracy of about 1000 ppm is sufficient to determine $\langle[B]\rangle$ to 100 ppm.

The mean radius of the beam can be determined from a study of the electron counting rate as a function of time immediately following the injection of the muons. Since the injection pulse length (5–10 nsec) is short compared to the rotation period (52 nsec), the initial counting rate will be modulated at the average rotation frequency $\langle\omega_R\rangle=\beta c\langle\rho\rangle$. Analysis of the fast modulation of the counting rate can be used to determine $\langle\rho\rangle$ to about 1000 ppm. The fast modulation dies away after several microseconds, due to the spread of radii present in the storage region. Additional measurements of the radius as a function of the storage time (made by mechanically restricting the ring aperture) show that the average radius varies by less than ±300 ppm from $T=3$ μsec to $T=190$ μsec (data for 20 μsec$\leq T\leq$190 μsec is used to determine ω_D). The final uncertainty in $\langle[\omega_p(H_2O)]\rangle$ is ±160 ppm.

Measurements were made for both μ^- and μ^+, with the μ^- contribution constituting a majority of the data. The final uncertainty in $\langle[\omega_D]\rangle$ obtained from a weighted average of the combined data was ±220 ppm. The final results of the 1968 experiment are

$$a_\mu=0.001166160(310)\ (270\text{ ppm}),$$

and

$$a_{\mu^-}-a_{\mu^+}=(50\pm75)\times10^{-8},$$

where the error in the latter result includes statistical error only (the radial distribution of stored muons is assumed to be identical for μ^+ and μ^-).

3.2 Resonance Experiments

3.2.1 *General Discussion*

The storage method employed in the resonance experiments of Gräff *et al.* and Dehmelt *et al.* is based on the confinement of low energy (0.01–10 eV) elec-

[20] The error in ω_D is proportional to $A^{-1}N_T^{-1/2}$, where N_T it the total number of counts recorded. Maximizing the producs A^2N_T therefore gives the optimum data rate.

trons in a Penning-gauge ion trap. The trap consists of a uniform axial magnetic field $\mathbf{B}=B_0\hat{z}$, and a superimposed electric quadrupole field generated by a pair of hyperbolic electrodes that surround the storage region (Fig. 3.12). The magnetic field confines the electrons radially, while the electric field confines them axially. With a voltage V_0 applied between the electrodes, the electrostatic potential in the trapping region is

$$V(r,z)=(V_0/r_0^2)(r^2/2-z^2), \tag{3.16}$$

where $r^2=x^2+y^2$. The vector potential is

$$\mathbf{A}(x,y)=(B_0/2)(-y\hat{x}+x\hat{y}). \tag{3.17}$$

The eigenvalues of the nonrelativistic Hamiltonian

$$\mathcal{H}=(\mathbf{p}+e\mathbf{A}/c)^2/2m_e-eV+(1+a)(e/2m_ec)\boldsymbol{\sigma}\cdot\mathbf{B} \tag{3.18}$$

have been calculated exactly (Sokolov and Pavlenko, 1967). They are

$$E(n_B,n_E,n_{EB},s_z)/\hbar=(n_B+\tfrac{1}{2})\omega_B+(n_E+\tfrac{1}{2})\omega_E-(n_{EB}+\tfrac{1}{2})\omega_{EB}-(1+a)\omega_0 s_z, \tag{3.19}$$

where n_B, n_E, and n_{EB} are integer quantum numbers, $s_z=\pm\frac{1}{2}$,

$$\omega_E=(2eV_0/mr_0^2)^{1/2},$$

$$\omega_B=\omega_0-\omega_{EB},$$

$$\omega_{EB}=\omega_0/2-(\omega_0^2/4-\omega_E^2/2)^{1/2},$$

and $\omega_0=eB/m_ec$. The motion in the trap consists of three decoupled motions: (1) cyclotron motion at the perturbed cyclotron frequency $\omega_B(2\pi\times 12$ GHz), (2) a slow drift of the cyclotron orbit center about z at the magnetron frequency ω_{EB} ($2\pi\times 70$ kHz), and (3) an axial oscillation at frequency ω_E ($2\pi\times 40$ MHz). The numerical values given are approximate frequencies for $B_0=4$ kG, $V_0=10$ V, and $r_0=0.8$ cm. For the experiments discussed, $\omega_E\ll\omega_B$, and therefore $\omega_{EB}\cong\omega_E^2/2\omega_0$. In the limit $V_0\to 0$, Eq. (3.19) reduces to the familiar expression for the Landau levels of an electron in a uniform magnetic field:

$$E(n_B,s_z)/\hbar=[n_B+\tfrac{1}{2}+(1+a)s_z]\omega_0.$$

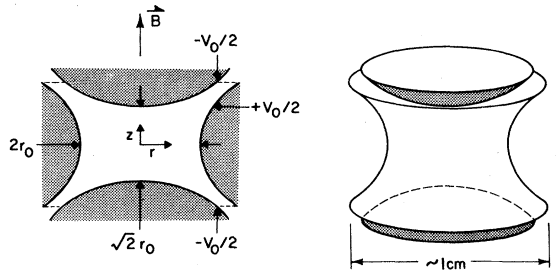

FIG. 3.12. The Penning-gauge trap.

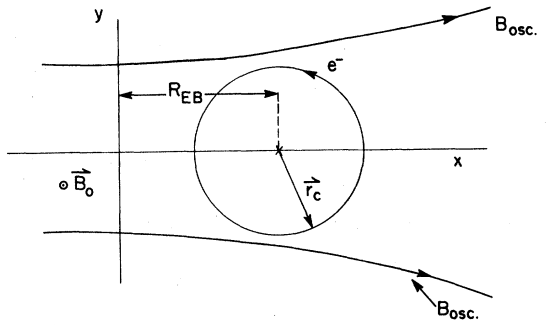

FIG. 3.13. Excitation of the difference frequency by an inhomogeneous rf field.

Transitions between eigenstates of $\mathcal{H}$ can be induced by appropriate types of oscillating electromagnetic fields. Three types of transitions of interest, and the required fields are:

(1) Cyclotron orbit transitions, $\Delta n_B=\pm 1$, $\omega=\omega_B$. This is an electric dipole transition, induced by a field of the type $\mathbf{E}\propto E_1\hat{x}\cos\omega_E t$.

(2) Spin flip transitions; $\Delta s_z=\pm 1$, $\omega=\omega_S=(1+a)\omega_0$. This is a magnetic dipole transition, induced by a uniform magnetic field of the type $\mathbf{B}\propto B_1\hat{x}\cos\omega_S t$.

(3) Direct g-2 transitions; $\Delta n_B=\pm 1$, $\Delta s_z=\mp 1$, $\omega=\omega_S-\omega_B=\omega_D'$. This is a simultaneous combination of (1) and (2), induced by a field of the type $\mathbf{B}_{\rm osc}=\{(\partial B_{\rm osc}/\partial x)(x\hat{x}+y\hat{y}-2z\hat{z})\cos\omega_D' t\}+$ const.

In case (3), the oscillating field must have a gradient perpendicular to $\hat{z}$ in order to induce the desired transition. To appreciate the reason for this, consider the case of a cyclotron orbit of radius r_c, located a distance R_{EB} from the z axis (Fig. 3.13). Since the x coordinate of the electron is given by $x=R_{EB}\cos(\omega_{EB}t+\theta)+r_c\cos\omega_B t$, the x component of the oscillator field in the electron rest frame (relativistic effects omitted) is

$$(B_{\rm osc})_x=(\partial B_{\rm osc}/\partial x)R_{EB}\cos(\omega_{EB}t+\theta)\cos\omega_D' t+(\partial B_{\rm osc}/\partial x)r_c\cos\omega_B t\cos(\omega_D' t+\varphi)+\text{const.}$$

Here $(\partial B_{\rm osc}/\partial x)$ is assumed constant and we take φ as the phase angle between the cyclotron motion and the difference frequency oscillator. The second term in this expression may be rewritten as

$$B_{\rm flip}\{\cos[(\omega_B+\omega_D')t+\varphi]+\cos[(\omega_B-\omega_D')t-\varphi]\}$$

with $B_{\rm flip}=\frac{1}{2}(\partial B_{\rm osc}/\partial x)r_c$. Thus the effect of the electron's rotation in a nonuniform field adds the frequency ω_B to the oscillator frequency ω_D to give a spin flip

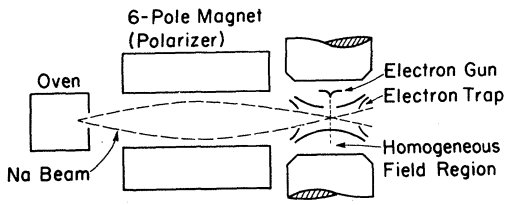

FIG. 3.14. Schematic diagram of the Mainz electron experiment.

transition at frequency $\omega_S=\omega_B+\omega_D'$. The spin flip occurs at a rate given by $(2\pi)^{-1}(g/2)(e/mc)B_{\text{flip}}$ sec^{-1}.

The perturbed cyclotron frequency ω_B is not equal to ω_0, except in the limit of zero applied trapping voltage. Therefore, ω_D' will be shifted from the "true" difference frequency $a\omega_0$. The effect is exactly analogous to the shift in a' (Eq. 3.11) due to a radial field in the precession experiments. As in these experiments, some sort of correction must be made for the effect of the electric trapping potential, either by extrapolation, or by direct measurement of ω_E or ω_{EB}. We also note that spin–orbit and relativistic terms are not included in Eq. (3.18). These terms have been considered in detail by Gräff, Klempt, and Werth (1969). They find that the net effect of these terms is to cause a fractional shift in the various transition frequencies that is of order T/m_ec^2, where T is the energy of the stored electrons. For the Mainz experiment, we have $T\sim 2$ eV, so that the shift is of order 4 ppm, which is small compared to the current accuracy (300 ppm). For the Washington experiment, we have $T\sim 0.01$ eV, so that relativistic effects are completely negligible at the 1 ppm level. Finally, we note that the orbital and spin motion in the Penning trap can be derived by straightforward application of the macroscopic equations of motion [Eqs. (3.4) and (3.5)]. Since the principal quantum number n_B is of order 10^3–10^4, there is no explicit need for a quantum mechanical solution. The quantum mechanical solution does, however, have the advantages of being both simple and exact. After having to deal with numerous methods of approximation to analyze the precession experiments, we find the concept of an exact solution to a spin motion problem to be quite novel!

In order to measure the anomaly, one measures ω_D' and either ω_S or ω_0 (ω_0 follows from direct measurement of ω_B). The details of the measurements and the appropriate corrections are discussed below.

3.2.2 *The Mainz Experiments*

The distinctive feature of the apparatus used in the experiments of Gräff and co-workers at Bonn[21] and Mainz is the molecular beam technique used to polarize the electrons and detect the induced spin transitions. The apparatus is shown in schematic form in Fig. 3.14.

A hot cathode located outside the trapping region is used to generate a pulsed electron beam which is arranged to traverse the central portion of the trap. These electrons ionize the residual gas molecules, thereby injecting low-energy (10 eV) electrons at the center of the storage region. The storage time that can be achieved in the Penning trap is determined primarily by scattering from the residual gas; for a pressure of 10^{-9} Torr and a field of 2.5 kG, storage times are of the order of several minutes. The number of electrons in the trap is monitored by a tuned circuit connected across the end electrodes of the ion trap. The resonant frequency ω_R of this circuit is chosen so that ω_R is slightly greater than ω_E. The circuit is weakly coupled to an external oscillator of frequency ω_R. After the desired storage time, the trapping voltage is increased linearly to a value such that $\omega_E>\omega_R$. At the time when $\omega_E=\omega_R$, the electrons extract energy from the tuned circuit and the voltage across the circuit decreases. The magnitude of the decrease is proportional to the number of electrons in the trap.

The electrons in the trapping region are initially polarized parallel to $\hat{z}$ by exchange collisions with transversely polarized Na atoms prepared by the usual molecular beam technique which incorporates a hexapole state-selecting magnet (Fig. 3.14). For an atomic beam flux of 10^{13} atoms cm^{-2} sec^{-1}, the electrons are polarized in about 10 milliseconds.

The spin orientation of the trapped electrons is monitored by means of the spin dependence of the inelastic excitation process

$$e^-(T)+\text{Na}(3S)\rightarrow e^-(T-2.1\text{ eV})+\text{Na}^*(3P). \quad (3.20)$$

The cross section for Eq. (3.20) is:

$$Q=(\tfrac{3}{4}Q_3+\tfrac{1}{4}Q_1)-\tfrac{1}{4}(Q_1-Q_3)pP, \quad (3.21)$$

where Q_3 is the cross section for a triplet (e^-, Na) collision, Q_1 is the singlet cross section, p is the atomic beam polarization, and P is the electron polarization (polarizations are measured parallel to $\mathbf{B}_0$). Since the cross section depends on P, the average rate of energy loss for the ensemble of trapped electrons will also vary as a function of P. Consequently, monitoring the energy distribution of the electrons provides a means for detecting changes in P induced by rf transitions. The specific method used is to lower the trap voltage adiabatically (with respect to the axial oscillations) to a value $V_0'=V_0/2$. This allows electrons with an energy greater than about 3 eV to escape. The trap voltage is then increased linearly in order to monitor the number of remaining electrons, using the method previously discussed. The voltage applied to the ion trap as a function of time is shown in Fig. 3.15. After the number of electrons is determined, a negative voltage pulse clears

[21] The experiment described in this section was performed at the Physical Institute of the University of Bonn. Current work is being performed at Johannes Gütenburg University at Mainz.

electrons from the trap prior to a repetition of the entire cycle.

The anomaly is determined by measuring the frequencies ω_S and ω_D'. The magnetic field necessary to induce the g-2 transition is realized experimentally by a pair of coils with current flowing in opposite directions. The resultant magnetic field gradient is 0.25 G/cm, corresponding to an average time for a spin flip of about 1 msec. A typical g-2 line is shown in Fig. 3.16. The fractional linewidth is 300 ppm, or about 4 kHz. A plot of the measured values of f_D' ($\omega_D'/2\pi$) as a function of the trap voltage V_0 (Fig. 3.17) shows a linear dependence of f_D' on V_0. A linear extrapolation to zero trapping voltage yields a value for the unshifted difference frequency f_D. This frequency is about 5000 ppm below the measured values. The spin resonance line is approximately 40 ppm in width. The line shapes of the g-2 and spin resonances are currently under investigation. In the preliminary account of the experiment, the linewidth of the g-2 transition limited the overall accuracy to 260 ppm in a. The final result of this experiment was $a_{e^-}=0.00115966(30)$.

3.2.3 *The Washington Experiments*

The ion trap used in the experiments of Dehmelt and co-workers is similar to that used in the Mainz experiments. The methods for polarizing and detecting the spin orientation of the trapped electrons are completely different. The detection method, the so-called "bolometric technique," is based on a measurement of the translational or axial temperature $\mathfrak{I}_z$ of the stored electron gas confined in the ion trap. The axial temperature is characteristic of the average kinetic energy associated with the axial oscillations in the trap; i.e.,

$$\tfrac{1}{2}k\mathfrak{I}_z=\tfrac{1}{2}m_e\langle v_z^2\rangle,$$

where k is Boltzmann's constant. Induced spin and cyclotron transitions result in changes in the spin and cyclotron temperatures associated with the corresponding degrees of freedom of the electron gas. Various relaxation processes transfer energy from the spin and cyclotron motions to the axial motion. Consequently,

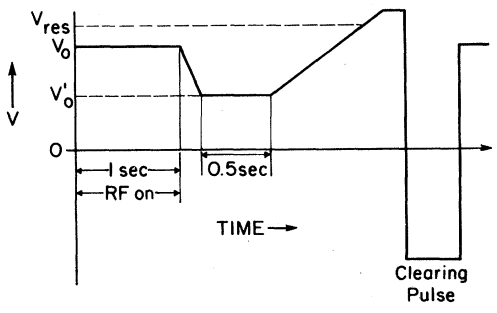

FIG. 3.15. Trap voltage applied in the Mainz experiment.

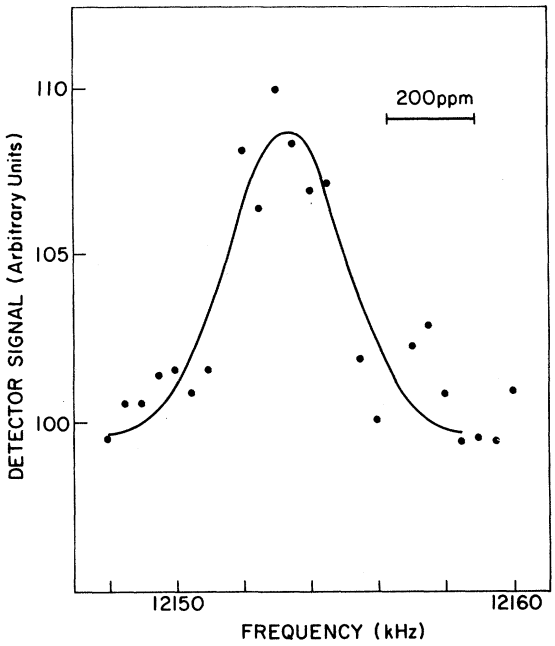

FIG. 3.16. Difference frequency resonance signal obtained in the Mainz experiment.

monitoring the axial temperature permits detection of the various resonances of Sec. 3.2.1.

The method for monitoring $\mathfrak{I}_z$ is as follows: The end electrodes of the ion trap are connected so as to form the capacity of an external tank circuit (Fig. 3.18). The voltage across this tank circuit is amplified by a low-noise tuned amplifier and detected by a square-law detector. The dc output of the detector is monitored. The tank circuit and amplifier are tuned to frequency ω_E. The axial motion of the trapped electrons induces a noise voltage V_N in the tank circuit (this voltage is in addition to the usual thermal noise from the amplifier input circuitry). Since V_N is proportional to v_z (Walls, 1970), the filtered output of the square law detector will be linearly related to $\mathfrak{I}_z$.

The combination of the electron gas and the external tank circuit can be analyzed as a thermodynamic system (Dehmelt and Walls, 1968). The internal degrees of freedom of the electron gas correspond to energy stored in spin orientation, cyclotron motion, and axial motion (Fig. 3.19). Only the axial motion is coupled to the tank circuit. Electron–electron collisions result in coupling between the cyclotron and axial modes. The natural coupling between the spin and cyclotron modes is extremely weak, since spin–spin forces are negligible at the low electron velocities involved. However, induced g-2 transitions result in a strong coupling (transfer of energy) between the spin and cyclotron modes. The following scheme can thus be used to detect g-2 transitions.

Consider the case of the electron gas initially in

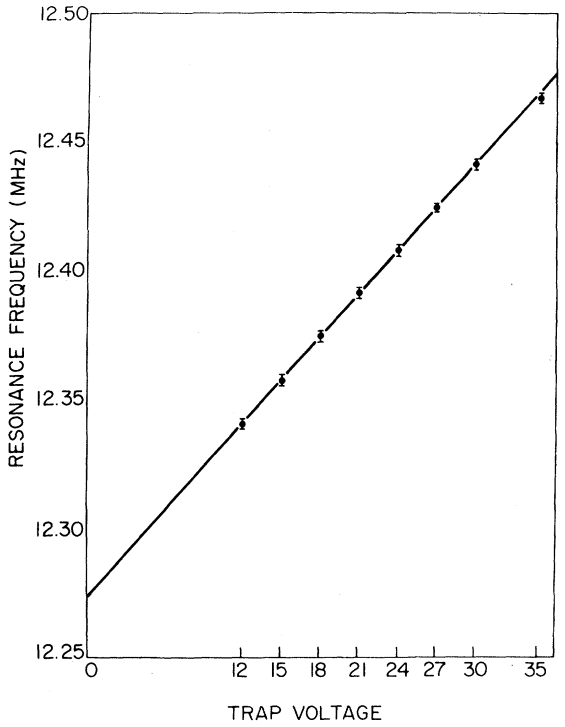

FIG. 3.17. Electric field extrapolation—Mainz.

thermal equilibrium with the tank circuit load resistor at temperature $\mathfrak{I}_0$. The relative numbers of electrons with spins parallel (+) and antiparallel (−) to **B** will exhibit a population asymmetry

$$n_-/n_+ = \exp(2\mu_e B_0/k\mathfrak{I}_0).$$

By applying a sufficiently strong transverse magnetic field at ω_S, the transition $+\leftrightarrow-$ can be saturated, and n_- and n_+ will approach equality. This corresponds to heating of the spin mode of the electron gas. If the ω_S field is now replaced with a field at ω_D', the increased energy stored in the spin mode can be coupled to the cyclotron mode, and ultimately detected using the bolometric technique. The experimental procedure for detecting a g-2 resonance consists of applying alternate intervals of the frequencies ω_S and ω_D' to the trapped electrons. Resonance is indicated by an increase in the average axial temperature of the electron gas.

Electrons are injected into the trap at the beginning of a data run by ionization of the residual background gas with a pulsed electron beam. Typically, 10^4 electrons are injected at one time. With $B_0=8$ kG, $V_0=14$ V, and a background pressure of 5×10^{-11} Torr, electron lifetimes in excess of *several days* can be obtained. The bolometric technique for interrogating the spin information is nondestructive. During a run one therefore makes repeated measurements using the same electrons! After injection, the radiative coupling between the tank circuit and the electron gas brings the gas temperature into equilibrium with the temperature of the tank circuit components with a time constant of about 0.2 sec. The time constant for internal thermal equilibrium between the cyclotron and axial modes is approximately 0.01 sec.

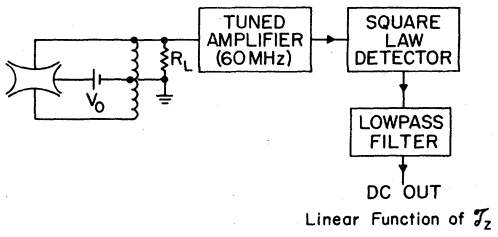

FIG. 3.18. Method for monitoring axial temperature in the Washington experiment.

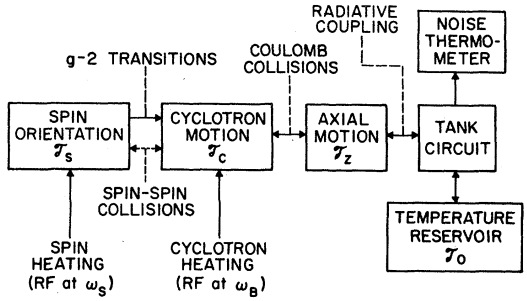

FIG. 3.19. Thermodynamic analysis of the Washington experiment.

Figure 3.20 shows a typical cyclotron resonance observed at a tank circuit temperature of 300°K. In addition to the resonance at ω_B, sidebands are observed at frequencies $\omega_B \pm n\omega_{EB}$, where n is an integer. The true cyclotron resonance can be separated from the sidebands by varying V_0. Only the resonance at the frequency $\omega_B+\omega_{EB}$ $(=\omega_0)$ will remain unshifted as V_0 is varied. The relative width of the cyclotron lines in Fig. 3.20 is approximately 1 ppm. Resonances with a width of 0.1 ppm have been observed at 80°K. The high resolution of this technique permits not only an accurate determination of ω_B, but also a direct measurement of ω_{EB}, and thus a direct measurement of ω_0, corrected for the presence of the electrostatic trapping fields.

A g-2 resonance obtained at 80°K with the same apparatus is shown in Fig. 3.21. The full width of the central peak of the resonance is approximately 30 ppm. The solid curve shown is a fit to the predicted

lineshape (Walls, 1970). The frequency obtained from the center of the g-2 resonance line is $\omega_D' = a\omega_0 + \omega_{EB}$. The true difference frequency is obtained by subtracting off the measured value of ω_{EB}, obtained either from the measurements of the spacing of the cyclotron sideband resonances, or from measurements of the axial frequency ω_E (recall $\omega_{EB} \cong \omega_E^2/2\omega_0$). Measured frequencies obtained in a typical data run are:

$$\omega_0/2\pi = 21{,}515.124(4) \text{ MHz},$$

$$\omega_E/2\pi = 58.58(1) \text{ MHz},$$

$$\omega_{EB}/2\pi = 0.0776(30) \text{ MHz},$$

$$\omega_D'/2\pi = 25.02660(20) \text{ MHz}.$$

The measured value of the anomaly is simply $a = (\omega_D' - \omega_{EB})/\omega_0$. The relative "correction" to the raw g-2 frequency (ω_D') is 0.07 MHz/25 MHz = 2800 ppm.

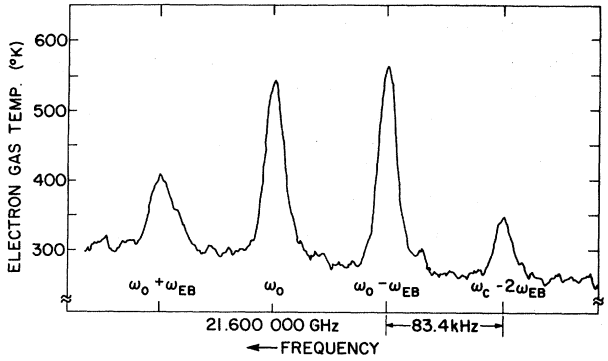

FIG. 3.20. Typical Washington electron cyclotron resonance.

The major uncertainty in the experiment reported by Walls is due to uncertainty in ω_{EB}. Accidental destruction of the ion trap prevented a detailed investigation of systematic effects associated with the cyclotron and g-2 resonances, and also prevented detailed lineshape studies. Consequently, the uncertainty in ω_{EB} was conservatively estimated to be 2 kHz, resulting in a final uncertainty in a of 70 ppm. The actual widths of the resonances, and the accuracy to which ω_{EB} could be determined in a single data run were considerably less, as noted above. The final result reported by Walls is $a_e^- = 0.001159580(80)$. It is expected that a significant improvement in accuracy will be possible in the future (see Sec. 4.2.2).

3.2.4 *The Stanford Experiment*

In the limit of zero electric potential, the energy eigenvalues of $\mathcal{H}$ [Eq. (3.18)] corresponding to the

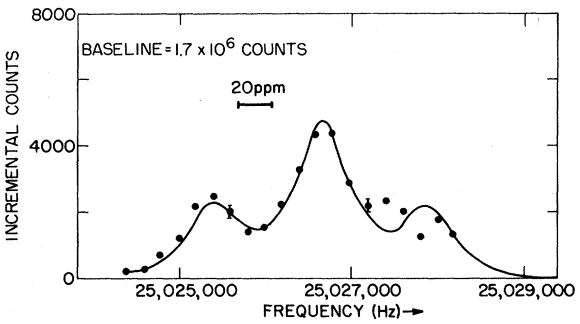

FIG. 3.21. Washington g-2 resonance signal.

state (n_B, s_z) become:

$$E(n_B, s_z) = \hbar\omega_0\{(n_B + \tfrac{1}{2}) + (1+a)s_z\} + (p_z^2/2m_e). \tag{3.21}$$

In the above, $n_B = 0, 1, 2, \cdots$, and $s_z = \pm\frac{1}{2}$. These states are the Landau levels of a spin $\frac{1}{2}$ particle in a magnetic field. The states corresponding to $n_B = 0$ and $n_B = 1$ can, in principle, be used to measure a_e^- to high accuracy by means of a method originally suggested by Bloch (1953). An experiment based on a modified form of Bloch's proposal is currently being attempted by Fairbank and his colleagues at Stanford.

The level structure of the lowest Landau levels, together with the transitions of interest, are shown in Fig. 3.22. The states are labeled with the notation (n_B, s_z). The energy of the ground state $(0, -\frac{1}{2})$ is approximately -10^{-8} eV per kG of magnetic field, while the energy of the first pair of higher states is approximately $+10^{-5}$ eV per kG of field. The transition $(1, -\frac{1}{2}) \leftrightarrow (0, -\frac{1}{2})$ is a cyclotron transition at frequency ω_0, while the transition $(0, \frac{1}{2}) \leftrightarrow (0, -\frac{1}{2})$ is a spin transition at frequency $\omega_S = (1+a)\omega_0$. Using $\hbar\omega_0 =$

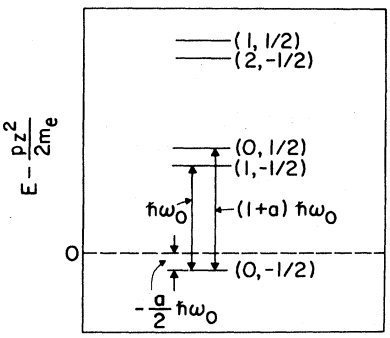

FIG. 3.22. The lowest Landau levels for an electron (not to scale).

TABLE II. Historical outline.

Date	Participants	Contribution
1921	Compton (C)	Suggests that ferromagnetism may be attributed to intrinsic magnetic properties of the electron. Also notes that the experiments of Barnett and Stewart imply $g>1$, and that this could be due to a nonuniform charge distribution within the electron.
1925	Uhlenbeck and Goudsmit (UG)	Postulate $S=\hbar/2$ and $g=2$ to explain alkali doublets and anomalous Zeeman effect.
1927	Dirac (D)	$S=\hbar/2$ and $g=2$ follow from the Dirac equation applied to an electron in electric and magnetic fields.
1947	Nafe, Nelson, and Rabi (NNR)	Hyperfine splitting in H and D is found to be at variance with the Dirac theory and the Fermi formula for hfs separation of S states.
1947	Breit (B)	Suggests that hfs discrepancy may be due to $g\neq 2$. Suggests effect is approximately $1+a/2$, so NNR (1947) data implies $a=0.006$. Later revision (1947) of calculation shows hfs shift is $1+2a$, so $a_e=0.0012$, in agreement with S (1948) and KF (1947).
1947	Kusch and Foley (KF)	Determine $a_e^-=0.00119(5)$ using an atomic beam technique to measure Zeeman splittings in Ga, In, and Na. First quantitative measurement of a_e.
1948	Schwinger (S)	Uses mass renormalization concept suggested by Kramers (1947) to eliminate divergences in QED. Calculates second-order correction to electron magnetic moment; $a_e=\alpha/2\pi+\cdots=0.00116$, in agreement with KF (1948) and NNR (1947).
1948	Luttinger (L)	Calculation of a for the special case of an electron in a magnetic field in the lowest ($n=0$) Landau level.
1948	Welton (W)	Semiclassical attempt to calculate a. Result: $a=-\alpha/2\pi$.
1949	Dyson (Dy)	Shows equivalence of Schwinger–Tomonaga and Feynman formulations of QED, and shows that lepton anomalies (as well as all quantities calculable via QED) can be calculated to arbitrary order in α. Gives precise "program" for calculating nth order contribution. Thus, for example, $a_e=A_e(\alpha/\pi)+B_e(\alpha/\pi)^2+C_e(\alpha/\pi)^3+\cdots$ Schwinger's calculation therefore gives $A_e=0.5$.
1949	Koba (K)	Refinement of W (1948). Result: $a=\alpha/2\pi$.
1949	Gardner and Purcell (GP)	Measure μ_p/μ_0. When multiplied by appropriate atomic g-factor ratios, this confirms S (1948) and KF (1947–8).
1950	Karplus and Knoll (KK)	Calculate $B_e=-2.97$, implying $a_e=0.001147$.
1953	Bloch (Bl)	Proposal for a g-factor experiment on electrons in the lowest Landau level of a magnetic field.
1953	Louisell, Pidd, and Crane (LPC)	First direct measurement of g_e; result $g_e=2.00\pm0.01$. Shows feasibility of a direct measurement of g_e using a Mott double-scattering technique with a magnetic field between scatterings.
1955	Mendlowitz and Case (MC)	Calculate effect of a uniform magnetic field on a Mott double-scattering experiment, showing that the effect can be used to measure g_e as in LPC (1953).
1956, 59	Franken and Liebes (FL)	Measure $\mu_p(\text{oil})/\mu_0$. When multiplied by known value of $\mu_e/\mu_p(\text{oil})$, this gives $a_e^-=0.001168(5)$, disagreeing with KK (1950).
1957	Suura and Wichman (SW)	Calculate $B_\mu-B_e=1.08(\alpha/\pi)^2$ (Rec'd. 24 January 1957).
1957	Petermann (P)	Calculates $B_\mu-B_e=1.08(\alpha/\pi)^2$ (Rec'd. 1 February 1957).
1957	Sommerfield (So)	Calculates $B_e=-0.32848(\alpha/\pi)^2$. Calculation of KK (1950) found to be in error. (Rec'd. 6 May 1957).
1957	Petermann (P)	Calculates $B_e=-0.32848(\alpha/\pi)^2$ (Rec'd. 17 August 1957).
1958	Hardy and Purcell (HP)	Refinement of FL (1956). Result: $a_e^-=0.0011561(10)$.
1958	Dehmelt (De)	Measures $g_J(\text{Na})/g_e=1.000026(30)$ for free thermal electrons (400°K) in argon buffer gas, using rf induced spin transitions. First demonstration of direct observation of spin transitions and measurement of a_e^- for free electrons. Result: $a_e^-=0.001116(40)$.
1959	Bargmann, Michel, and Telegdi (BMT)	Analyze spin motion of a relativistic particle in electric and magnetic fields.
1961	Schupp, Pidd, and Crane (SPC)	Modify LPC (1953) technique to measure a directly with free electrons. Result: $a_e^-=0.0011609(24)$ in agreement with B_e as calculated by P (1957) and So (1957).

TABLE II (*Continued*)

Date	Participants	Contribution
1961	Ford and Hirt (FH)	Alternate approach to spin motion analysis of a relativistic particle in electric and magnetic fields.
1961	Charpak, Farley, Garwin, Muller, Sens, Telegdi, and Zichichi (CFT)	First direct measurement of a_μ. Indirect measurements of g_μ are omitted from this table. References to such work can be found in CF (1962). Result: $a_\mu{}^+ = 0.001145(22)$ agrees with theory.
1962	Charpak, Farley, Garwin, Muller, Sens, and Zichichi (CF)	Refinement of CFT (1961). Result: $a_\mu{}^+ = 0.001162(5)$. Final results were published in 1965.
1962	Bloom and Erdman (BE)	Proposal for a "transverse Stern–Gerlach" experiment to measure a_e by a direct resonance technique.
1962	Rastall (R)	Transitions of the type proposed by BE (1962) are shown not to occur in the proposed field configuration.
1963	Byrne (By)	Further analysis of BE proposal, with the conclusion that a direct g-2 resonance is possible for a proper combination of static and rf fields.
1963	Wilkinson and Crane (WC)	Refinement of SPC (1961). Result: $a_e{}^- = 0.001159622(27)$, in excellent agreement with 1963 theory of $a_e = 0.001159615$.
1963	Farago, Gardner, Muir, and Rae (FG)	Direct measurement of a_e. Result: $a_e{}^- = 0.001153(23)$.
1965	Drell and Pagels (DP)	Estimate of C_e using dispersion theory. Result: $C_e = 0.15$ suggests sixth-order coefficient will have little effect on theoretical value of a_e.
1966	Rich and Crane (RC)	Extension of SPC (1961) technique to measure $a_e{}^+$. Result: $a_e{}^+ = 0.001168(11)$ shows e^- and e^+ g factors agree to 10 ppm, as predicted by TCP invariance.
1966	Farley, Bailey, Brown, Gresch, Jöstlein, VanderMeer, Picasso, and Tannenbaum (FB)	Measurement of $a_\mu{}^-$ using a muon storage ring. Result: $a_\mu{}^- = 0.001165(3)$.
1968	Parsons (P)	Refinement of DP (1965) dispersion theory estimate of C_e. Result: $C_e = 0.13$.
1968	Rich (R)	Recalculation of a_e from data of WC (1963), using corrected orbit motion theory and data analysis procedures. Corrected result is $a_e{}^- = 0.001159557(30)$, while 1968 theoretical result is now $a_e = 0.001159641$, due to revision of the accepted value of α.
1968	Bailey, Bartl, Von Bochmann, Brown, Farley, Jöstlein, Picasso, and Williams (BB)	Refinement of FB (1966). Final result: $a_\mu{}^- = 0.00116616(31)$, compared to $a_\mu(\text{theory}) = 0.0011656(1)$. Experimental result (TCP check): $g_\mu{}^- - g_\mu{}^+ = (50 \pm 75) \times 10^{-8}$.
1968	Gräff, Major, Roeder, and Werth (GMRW)	Direct observation of spin and cyclotron resonances of free thermal electrons in Penning configuration ion trap. Result: $a_e{}^- = 0.001159(2)$.
1968	Dehmelt and Walls (DW)	Detection of electron cyclotron resonance using "bolometric" technique on thermal electrons confined in a Penning ion trap.
1969	Gräff, Klempt, and Werth (GKW)	Refinement of GMRW (1968) to measure $a_e{}^-$ directly. Result: $a_e{}^- = 0.001159660(30)$. First reported observation of g-2 transitions by means of rf absorption.
1969	Gilleland and Rich (GR)	Refinement of RC (1966). Result: $a_e{}^+ = 0.0011602(11)$ or $g_e{}^- = g_e{}^+$ to 1 ppm.
1969	Henry and Silver (HS)	Correction to spin motion in WC (1963) experiment. Final revised result is $a_e{}^- = 0.001159549(30)$.
1969	Gourdin and de Raphael	Calculation of hadronic vacuum polarization contribution to a_μ. Result: $(\delta a_\mu)_{\text{strong}} = (65 \pm 5) \times 10^{-9}$
1970	Walls (Wa)	Preliminary measurement of a_e using bolometric technique of DW (1968). Result: $a_e{}^- = 0.001159580(80)$.
1971	Wesley and Rich (WR)	SPC (1961) technique extended to high fields. Result: $a_e{}^- = 0.001159657.7(3.5)$ or $C_e = 1.68 \pm 0.33$. Fails to confirm revised WC result.
1969–1971	Mignaco and Remiddi; Aldins, Kinoshita, Brodsky, and Dufner; Brodsky, and Kinoshita; Levine and Wright	Calculation of various Feynman diagrams for C_e and C_μ. Combined results give $C_e = 1.49 \pm 0.2$, $C_\mu = 21.8 \pm 1.3$ in agreement with experiment.

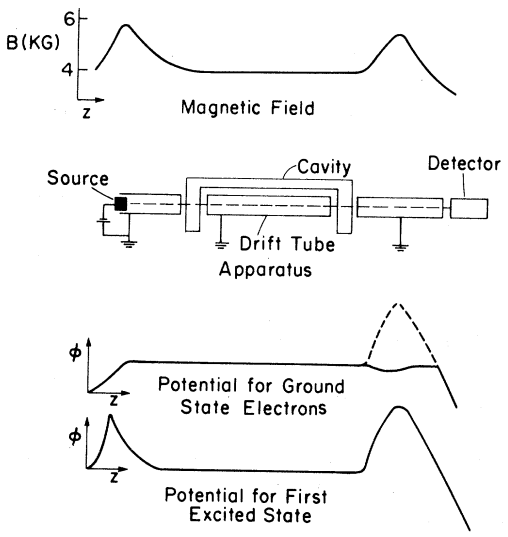

FIG. 3.23. The Stanford electron–positron experiments.

$2\mu_B B_0$, Eq. (3.21) can be rewritten as:

$$E(n_B, s_z) = \mu(n_B, s_z) B_0$$
$$= \{2(n_B+\tfrac{1}{2})\mu_B + 2(1+a)s_z\mu_B\} B_0 + (p_z^2/2m_e),$$

where $\mu(n_B, s_z)$ can be identified as the total magnetic moment of the state (n_B, s_z). The total magnetic moment is the sum of the orbital moment $2(n_B+\frac{1}{2})\mu_B$ and the intrinsic electron moment $\pm(1+a)\mu_B$. Note that the magnetic moment of the ground state $(0, -\frac{1}{2})$ is negative and small $(=-a\mu_B)$ as opposed to the larger positive moments of the higher states. This distinction provides a basis for measurement of the frequencies ω_0 and ω_S, as described below.

The components of the experiment are shown in Fig. 3.23. The entire apparatus operates at liquid helium temperatures, the magnetic fields being generated by superconducting solenoids. A 0.1-msec pulse of low-energy electrons ($\sim\frac{1}{2}$ eV) is produced by a tunnel cathode (Knight, 1965). An appreciable fraction (about one electron per pulse) are in the ground state. The cathode is located in a region of inhomogeneous magnetic field ($B\cong 6$ kG). The axial gradient causes the electrons to experience a force $F_z=\mu_z(\partial B_z/\partial z)$. Consequently, the ground state electrons are decelerated slightly as they drift away from the cathode. Electrons in higher-energy states, i.e., those with much larger positive moments, experience a strong acceleration away from the cathode. The initial axial energy of the ground state electrons is of the order of 10^{-8} eV. The axial energy increase for those of higher energy is at least 10^{-5} eV for a 2 kG decrease in magnetic field. The electrons drift into a region of homogeneous magnetic field (4 kG) approximately 1 meter long. Those in higher states move through this region in less than 0.3 msec, while the slower ground state electrons require up to 30 msec. Consequently, ground state electrons can be identified by their time of flight through the apparatus.

The drifting electrons pass through the ends of a "U-shaped" microwave cavity located in the homogeneous region (Fig. 3.23). A second region of higher magnetic field separates the output end of the cavity from an electron multiplier detector. For electrons in the ground state, the high field region acts as a slight axial potential trough, but for the others, it acts as a potential barrier. Therefore, electrons that undergo a transition from the ground state to a higher state will be unable to reach the detector. Thus, if the microwave frequency in the cavity is close to either ω_0 or ω_S, the counting rate at the detector will decrease.

The phase of the microwave field in either end of the cavity differs by exactly π. Consequently, an electron that undergoes a cyclotron or spin transition in the first section of the cavity will undergo an exactly opposite transition if the average cyclotron or spin frequency of the electron in the drift region is exactly equal to the applied microwave frequency. For this condition, the counting rate will exhibit a maximum. The observed resonance line will therefore consist of a broad cavity resonance line, with a much narrower maximum in the center. The method is identical to the Ramsey separated field method employed in molecular beam experiments. Indeed, the entire apparatus is very similar in concept to a molecular beam machine.

The linewidth of the central spin and cyclotron resonances is expected to be approximately $1/\pi N$, where N is the total number of cyclotron or spin rotations between the ends of the cavity. For a drift time of 10 msec and a field of 4 kG ($\omega_0\cong 10$ GHz), this gives a relative linewidth of about 3×10^{-9}. Even without splitting the line, this would permit a determination of **a** to about 3 ppm. Knight (1965) has proposed that the resonance line may be split by about $1:10^3$. If so, this would permit a measurement of **a** to 0.01 ppm. Achieving this accuracy would, however, place extreme requirements on the experimental apparatus.

Some of the difficulties are as follows: in view of the data rates obtained with a preliminary version of the apparatus (Knight, 1965) which did not incorporate the rf cavity, the running time for a 0.01 ppm g-2 measurement is estimated to be about 4 days. During the course of the data run, both the magnetic field and the microwave frequency must be stabilized to $1:10^{11}$. The proposed field stability is to be achieved through the use of superconducting solenoids operated in the persistant current mode, and through the use of superconducting shields. The necessary frequency stability is within the state of the art, but both field and frequency stability requirements are expected to present problems.

Obtaining a suitable microwave field configuration within the cavity may also be difficult. The cyclotron resonance is an electric dipole transition, while the

spin resonance is a magnetic dipole transition. For equal field strengths in the cavity, the transition rates will differ by a factor of c^2, where c is the velocity of light. Assume that in the cavity, we have $E_{rf}=B_{rf}$, and that in order to obtain a given signal-to-noise ratio for the cyclotron resonance, we use a cavity power input P_0 at ω_0. In order to obtain the rf magnetic field required to give an equal signal-to-noise ratio for the spin resonance, we need a power input $P_0'=c^2P_0$ at frequency ω_S. In addition to the desired rf magnetic field, this gives us a very intense rf electric field. Since ω_0 and ω_S differ by only 1100 ppm, and the cavity resonances are approximately 1 ppm in width, the intense electric field will tend to excite cyclotron transitions, in spite of the fact that the applied frequency is not ω_0. Any spurious harmonic content at frequency ω_0 will further aggravate the problem. Consequently, spurious excitation of the cyclotron resonance may perturb or completely obscure the much weaker spin resonance. It will therefore be necessary to operate the cavity in a mode in which the rf electric field is much weaker than the rf magnetic field, in order to make the spin and cyclotron transition probabilities more nearly equal.

Finally, we note that the effects of electric fields must be shown to be negligible. Preliminary tests show that the electric fields on the axis of the OFHC copper drift tube used to enclose the drift region have no significant effect on the axial motion of 10^{-8} eV electrons. It remains to be demonstrated however, that the spin and cyclotron frequencies are independent of the conditions inside the drift tube to the projected accuracy of the experiment.

Work is currently in progress at Stanford towards detecting the induced transitions, and on a technique for thermalizing positrons from a beta source (Kincaid, 1970). If reasonable numbers of ground state positrons can be produced, it may then be possible to measure a_{e^+} to much higher accuracy than is currently possible.

3.3 Critical Analysis

In this section, we will discuss some of the comparative advantages and difficulties associated with the experiments described in the previous sections of this chapter. We will confine our attention to those factors which influence the over-all uncertainty and significance of the final experimental values. It should be noted that the precession experiments have reached a more refined state of development than the resonance experiments, and this fact should be kept in mind throughout the discussion.

There are four general problem areas associated with current g-2 experiments: (1) magnetic field measurement and averaging, (2) line shape considerations, (3) relativistic corrections, and (4) electric field extrapolation or measurement. The field averaging problem applies only to the precession experiments, while the lineshape problem is significant only in the resonance experiments. Relativistic corrections are or will be necessary in several current experiments. The electric field problem is common to both the precession and resonance techniques, and ultimately constitutes the most probable source of significant systematic error.

3.3.1 *Field Measurement and Averaging*

As we have noted above, this problem is specific to the precession experiments. Point-by-point measurement of the magnetic field using NMR in itself presents no difficulty. However, since the trapping field is inhomogeneous, measurement of the distribution of the particles in the trapping region and further calculation is necessary to determine the average magnetic field experienced by the stored particles. In the case of the muon experiments, a simple azimuthal average, combined with a measurement of the average orbital radius is sufficient. For the Michigan electron experiments, the nonuniform axial motion must be considered. In either case, well-defined procedures have been developed for calculating the time- and ensemble-average field in terms of directly observable experimental quantities. Although the details of these procedures are somewhat complex, the methods are essentially straightforward. In addition, various systematic tests are available to check the assumptions on which the calculations are based. In the electron experiments, the average magnetic field can be determined to an over-all accuracy of about 1:15 of the relative well depth; i.e., for a 50 ppm ($=\pm 25$ ppm) well, the average field can be established to about ± 1.5 ppm. In the muon experiments, the average field variation over the effective aperture of the storage ring is ± 1000 ppm, while the final field uncertainty is ± 160 ppm, equivalent to a factor of six reduction in over-all uncertainty. We note that the effective reduction in the field uncertainty in the electron experiments is about a factor of 7,[22] nearly identical to that achieved in the muon experiment, using an entirely different technique. Thus a reduction in overall field uncertainty by about a factor of ten appears to be both typical and practical. A detailed analysis of the most recent electron experiment (Wesley, 1970; Wesley and Rich, 1971) indicates that less than half the final field error is due to systematic uncertainty associated with the field averaging process. While it is conceivable that more accurate distribution measurements might permit "splitting" the experimental field inhomogeneity by a further factor of 2 to 5, the possibility for significant systematic error can be expected to increase substantially. As long as the effective reduction in the

[22] For a magnetic field $B_z=B_0+B_1(z/L)^2$, $[B]=B_0+\frac{1}{2}B_1$ for a particle oscillating between turning points at $z=\pm L$. Thus, one obtains a two reduction in field uncertainty without further knowledge of the electron distribution.

field inhomogeneity is limited to less than a factor of ten, the systematic error introduced is not significant.

The necessity to evaluate the average magnetic field is, of course, not present in the resonance experiments, since the average field is measured directly, in terms of either the average cyclotron or spin frequency of the stored electrons. Since the measurement can be made under very similar conditions to those used to determine the difference frequency, field maps and measurements of the electron distribution are not required.

3.3.2 *Lineshape Theory*

The ultimate accuracy of a resonance experiment is limited by the width of the resonance lines and the precision with which the line can be split. Difference frequency resonances currently observed have exhibited widths of from 10 to 100 ppm. Since the resonance experiments reported to date have been preliminary demonstrations of new techniques, rather than concerted precision measurements, detailed line shape theories have not been developed or applied, and no attempt has been made to split the lines to a high degree of accuracy. Unless the linewidth can be reduced to a few ppm, future experiments will require formulation and verification of a satisfactory lineshape theory.

3.3.3 *Relativistic Corrections*

So far, relativistic corrections have been important only in the Michigan experiments. The total correction is of approximately the same magnitude as the overall experimental uncertainty, and the systematic uncertainty in the correction is negligible. Relativistic corrections for the resonance experiments are of the order of T/m_ec^2. Since, in the Mainz experiments, the electron energy must be greater than about 5 eV to permit use of their spin analysis technique, relativistic effects will become significant at the 10 ppm level. In the Washington experiments, the electron energy is about 0.02 eV, and can in principle be reduced by perhaps an additional factor of twenty. Therefore, relativistic corrections in this experiment can be neglected at even the 0.1 ppm level!

3.3.4 *Electric Field Extrapolation and Measurement*

In the Michigan electron experiments, shifts in the difference frequency due to stray electric fields in the trapping region present both a problem in the interpretation of the data, and a potential source of systematic error. Similar problems are present in the resonance experiments, where electric fields are intentionally introduced in order to permit confinement of the electrons. In each case, an extrapolation or measurement procedure is used to correct for the effects of the electric field shift. If systematic error is to be avoided, it is necessary to give careful consideration to the verification of the assumptions on which the extrapolation and measurement procedures are based.

The electric field extrapolation procedure used in the Michigan experiments is perhaps the portion of the experiment that is most open to criticism. The difficulty does not lie in the extrapolation *per se*, but rather in the assumptions that must be made to interpret the limited amount of experimental data that is available. Specifically, one must assume that $\langle[E_r]\rangle$ is independent of X, and is constant over the entire series of data runs (several weeks). If these assumptions are valid, then a linear extrapolation of the measured dependence of $a'(X)$ to $X=0$ will yield the "true" value of a.

No direct means for measuring either E_r or $\langle[E_r]\rangle$ within the experimental region has been devised. Consequently, the only means available to measure $\langle[E_r]\rangle$ is by observing the dependence of a' on X. Thus, direct tests of the validity of the various assumptions made above are not possible, since the electric field "measuring" procedure is intimately connected with the assumptions that one is trying to verify.

Although a definitive test is not possible, various theoretical speculations and experimental tests can be used to estimate the systematic error introduced by the extrapolation procedure. The hypotheses that a' is a linear function of X, and that a' is constant from run to run at a given value of X, can be tested statistically. The sensitivity of these tests to systematic effects which are small compared to the error in the individual measurements that comprise the test is low. One can however, rule out any large effect. Experimentally, one can also measure a' as a function of various experimental parameters, particularly those of a "suspicious" nature. For example, parameters such as the number of trapped electrons and residual gas pressure might be expected to influence the electric fields from space charge, residual gas ionization, or charging of dielectric films on the inner surfaces of the trapping region. The magnitude and possible variation of the fields from these sources can also be estimated theoretically. The net result of these tests and speculations suggests that the systematic error introduced by the electric field extrapolation is small compared with the remaining sources of error in the experiment. In the most recent Michigan experiment, the systematic error (mainly from electric fields) is estimated to be about 1 ppm, out of a total error of 3 ppm.

The effect of electric fields in the muon experiments is expected to be negligible because of the magnitude of the magnetic field employed. For any reasonable electric fields ($\sim$1 V/cm), the shift in ω_D is expected to be less than about 10 ppm.

The electric fields intentionally introduced in the resonance experiments are of the order of 1 V/cm. The shift in the difference frequency is therefore quite large. The measured values of ω_D' are shifted from $a\omega_0$ by 5000 to 15 000 ppm in the Mainz experiment, and by

2800 ppm in the Washington experiment. The amount of extrapolation or correction required is therefore two to three orders of magnitude greater than that made in the Michigan experiments. Again, there is no fundamental objection to such an extrapolation, but considerable care must be taken to verify the underlying assumptions. If the potential in the trapping region is quadratic in r and z, and due solely to the applied trapping voltage, then the effect of the electric field can be corrected for by a linear extrapolation to zero voltage (Mainz) or a direct measurement of the magnetron frequency (Washington). In the presence of a nonquadratic potential, due to either space charge or nonuniform surface potentials on the trapping electrodes, the expressions for the various frequencies of motion in the Penning trap given in Sec. 3.2.3 must be modified. In the presence of an additional electric field E^e, the shifted frequencies (denoted by the notation $'$) become (Walls, 1970):

$$\begin{aligned}
\omega_E'^2 &= \omega_E^2 - (e/m_e)(dE_z^e/dz), \\
\omega_B' &= \omega_0 + \omega_{EB}', \\
\omega_{EB}' &= \omega_{EB} + (c/B)(E_r^e/R_{EB}), \\
\omega_D'' &= a\omega_0 + \omega_{EB} + (c/B)(dE_r^e/dr), \qquad (3.22)
\end{aligned}$$

where R_{EB} is the magnetron radius. Unless $dE_r^e/dr = E_r^e/R_{EB}$, the shift in the difference frequency is not equal to the observed magnetron frequency, and extrapolation of ω_D'' to $V_0=0$ does not yield $a\omega_0$. Also ω_{EB}' is no longer independent of the magnetron radius of the stored electron. Therefore, if the applied rf fields are not uniform, additional complications will be introduced into the lineshape theory. Walls (1970) estimates that the fractional shift in ω_{EB} due to the space charge field from 10^4 stored electrons could be as large as 10^{-2}, but is more probably of order 10^{-3}–10^{-4}. The effect is certainly not significant at the 100 ppm level, but may be important in more accurate measurements, where careful studies of ω_D'' and ω_{EB}' as a function of the number of trapped electrons will be necessary.

3.4 Comparison of Theory and Experiment: Current Status of the Lepton *g*-Factors

Within the limits of accuracy achieved with current experimental techniques, there is no significant evidence for a disagreement between QED calculations and measurements of the lepton g-factor anomalies. The currently accepted theoretical values and most recent (and accurate) measurements are:

$$\begin{aligned}
a_e(\text{theory}) &= 0.5(\alpha/\pi) - 0.32848(\alpha/\pi)^2 + (1.49\pm0.2)(\alpha/\pi)^3 \\
&= (1\,159\,655.3\pm2.5)\times10^{-9} \qquad (1.9 \text{ ppm}), \qquad (3.23)
\end{aligned}$$

(Levine and Wright, 1971)

$$a_{e^-}(\text{expt}) = (1\,159\,657.7\pm3.5)\times10^{-9} \qquad (3.0 \text{ ppm}), \qquad (3.24)$$

or

$$a_{e^-}(\text{expt}) - [0.5(\alpha/\pi) - 0.32848(\alpha/\pi)^2] = (1.68\pm0.33)(\alpha/\pi)^3, \qquad (3.25)$$

(Wesley and Rich, 1971).

$$a_{e^+}(\text{expt}) = (1\,160\,200\pm1100)\times10^{-9} \qquad (950 \text{ ppm}), \qquad (3.26)$$

$$a_{e^+}(\text{expt}) - 0.5(\alpha/\pi) = (-0.22\pm0.20)(\alpha/\pi)^2, \qquad (3.27)$$

(Gilleland and Rich, 1969).

$$\begin{aligned}
a_\mu(\text{theory}) &= 0.5(\alpha/\pi) + 0.76578(\alpha/\pi)^2 + (21.8\pm1.3)(\alpha/\pi)^3 + (65\pm5)\times10^{-9} \quad \text{(hadronic vacuum polarization)} \\
&= (1\,165\,878\pm17)\times10^{-9} \qquad (15 \text{ ppm}), \qquad (3.28)
\end{aligned}$$

$$a_\mu(\text{expt}) = (1\,166\,160\pm310)\times10^{-9} \qquad (270 \text{ ppm}), \qquad (3.29)$$

$$a_\mu(\text{expt}) - [0.5(\alpha/\pi) + 21.8(\alpha/\pi)^3 + 65\times10^{-9}] = (0.82\pm0.06)(\alpha/\pi)^2 \qquad (3.30)$$

(Bailey *et al.*, 1968).

Note that in Eq. (3.30), it is necessary to include the sixth-order electromagnetic and the hadronic vacuum polarization contributions to a_μ on the right-hand side in order to accurately compare the current experi-experimental and theoretical values of the fourth-order coefficient.

The accuracy of the CERN measurement (270 ppm) is roughly comparable to the sum of the sixth order and hadronic contributions to a_μ. Therefore, in interpreting the results, one can either think in terms of a 10% check of the fourth-order contribution, or a preliminary check of the combined sixth-order and hadronic contributions. The choice is entirely arbitrary.

Comparisons of lepton–antilepton g factors indicate

no deviations from the predictions of TCP invariance at the 1 ppm level. The experimental results are

$$a(e^-)-a(e^+)=(-543\pm1100)\times10^{-9},$$

or

$$[g(e^-)-g(e^+)]/g(e)=(-0.54\pm1.1)\text{ ppm} \quad (3.31)$$

(Gilleland and Rich, 1969; Wesley and Rich, 1971), and

$$a(\mu^-)-a(\mu^+)=(500\pm750)\times10^{-9}$$

(statistical error only), or

$$[g(\mu^-)-g(\mu^+)]/g(\mu)=(0.5\pm0.75)\text{ppm} \quad (3.32)$$

(Bailey *et al.*, 1968).

In its purely numerical aspects, the agreement between theory and experiment, as noted above, is excellent. However, in another sense, this agreement is less satisfactory than it appears to be. We note that for each specific lepton, the experimental value is derived from a single experiment that is significantly (a factor of ten) more accurate than any other available independent measurement. In most cases, the technique used is a refinement of that used in previous measurements. Consequently, it has not been possible to test for the presence of systematic errors specific to a certain experiment or family of experiments by comparing the results of several independent measurements, each with a similar level of accuracy. Such a comparison would be highly desirable, in view of the difficulties involved in estimating unknown systematic errors. For this reason, it is important that the accuracy of the electron resonance experiments be extended to the ppm level, so as to provide an independent check of the precession measurements of a_{e^-}. Unfortunately, an analogous technique does not appear feasible in the case of the muon. We note, however, that a precession experiment using somewhat different parameters than those used by the CERN group is now being considered at Yale (Sec. 4.3).

IV. PROSPECTS FOR FUTURE PROGRESS

4.1 Theory

The theory of quantum electrodynamics as it is presently formulated can, in principle, be used to calculate the electromagnetic contribution to the lepton anomalies to arbitrary precision. The calculational procedure, although complex, is well defined. Therefore, calculating the eighth- and higher order contributions to **a** is simply a matter of "perseverance," i.e., enough computer time. The usefulness of such a calculation would, however, depend on a number of factors, including the accuracy achieved in future anomaly measurements, uncertainty in α, and for the muon, better knowledge of the hadronic contributions to a_μ. As a point of reference, $(\alpha/\pi)^4$ is 0.02 ppm of **a**. It is therefore quite conceivable that the eighth-order contribution to **a** may be as large as 0.1 ppm for the electron, and 1 ppm for the muon (recall $C_\mu\cong20$). At the present time, uncertainty in the *known* hadronic contributions limits the ultimate accuracy of a_e to about 0.001 ppm, and the accuracy of a_μ to about 5 ppm. Thus, it appears that an eighth-order calculation would be of interest for the electron. For the muon, it would be of limited value unless hadronic effects are more accurately known. Of course, one can assume QED to be valid and use such a calculation, in conjunction with more accurate experiments to measure the hadronic contribution to a_μ. In part, such a consistency check is the motivation for the new muon experiments (see Sec. 4.3).

At the present time, the 1.5 ppm uncertainty in α contributes approximately half the uncertainty in the numerical value for a_e (theory). However, it appears quite likely that a sub-ppm value of α independent of QED will be available in the next few years. Assuming that more exact theoretical calculations and experimental measurements of the anomaly are available, such a value will provide the key for their comparison.

4.2 Electron Experiments

4.2.1 *Precession Experiments*

There appears to be no fundamental reason why the Michigan g-2 technique cannot be extended to accuracies better than 1 ppm. A further increase in magnetic field and electron energy appears to offer the means to reduce both statistical error and systematic error from electric fields (recall that for electric fields $\delta a/a\sim\langle[E_r]\rangle/\beta\gamma^2B$). In a preliminary study, we have considered an experiment incorporating a 10 kG field, a 10 ppm trap, and a nominal electron energy of 1 MeV. These parameters differ by roughly an order of magnitude from those used in the latest Michigan experiment. As a result several qualitatively new problems appear. We estimate, however, that a considerable improvement over the previous accuracy may be possible if a conventional electron g-2 precession experiment is done at this high value of magnetic field. In addition one of us (A.R.) has recently noted that an experiment done at 10 kG but using a *uniform* magnetic field and dc electric field for trapping may be feasible. With proper electrode arrangement the $\langle[E_r]\rangle/\beta\gamma^2B$ term in Eq. (3.9) can be reduced to less than 0.2 ppm, consistent with a reasonable trap depth! The advantage of not having to correct for field nonuniformity is obviously considerable. Thus, we see that order-of-magnitude improvements in experimental accuracy using extensions of the current Michigan g-2 scheme may indeed be possible and new experiments are now under consideration.

4.2.2 *Resonance Experiments*

The resonance experiments also appear to offer promise for breaking the 1 ppm barrier in measurements of a_e. In particular, the apparatus currently being used in the Washington experiment should be capable of a measurement at the 10 ppm level in the near future. Unless unexpected problems arise, it seems reasonable to expect that a second generation version of the apparatus (perhaps operating at a much higher magnetic field) may reach or surpass an accuracy of 1 ppm. It should be pointed out again that, subject to the considerations discussed in Sec. 3.3.4, the Washington technique offers the possibility for a direct measurement of the effects of electric fields present in the trapping region. Consequently, the possibility for systematic error from electric fields may be significantly reduced in comparison to experiments that are forced to rely on extrapolation procedures.

The spin detection method and extrapolation procedure used in the Mainz experiment may prove to be the fundamental limiting factors in that work. The spin detection technique prevents reduction of the electron energy below about 3 eV. Consequently, relativistic corrections and line broadening become significant at the 10 ppm level. The extrapolation procedure, at least in its present form, may not fully correct for electric fields from contact potential differences and space charge. The ultimate accuracy of the method is therefore somewhat unclear. It does seem reasonable to expect that considerable improvement over the current level of 250 ppm will be possible.

The potential accuracy of the Stanford experiment is even more uncertain. In principle, a 0.01 ppm measurement is possible. However, since the rf transitions have not, as of yet, been observed, detailed speculation seems premature.

4.3 Muon Experiments

In muon g-2 experiments incorporating a conventional storage ring, the field inhomogeneity necessary to achieve vertical focusing presents the greatest obstacle to improved accuracy. If a storage ring is to have reasonable angular acceptance, and if particle losses owing to betatron resonances are to be avoided, the field index n (defined in Sec. 3.1.4) cannot be made less than about 0.1. For a 5% spread in the momentum of the injected muons, this value of n effectively limits knowledge of the average magnetic field to about 100 ppm (recall that $\Delta B/B = n\Delta\rho/\rho = n\Delta p/p$, where p is the muon momentum). However, instead of trying to determine the average orbit radius to great accuracy, one can take the alternate approach of making ω_D independent of storage radius. Note that, in Eq. (3.6), the coefficient of the $\boldsymbol{\beta} \times \mathbf{E}$ term (which is responsible for the electric field shift) is $(1/\beta^2\gamma^2 - a)$. Thus, for $\beta^2\gamma^2 = a^{-1}$, or $\gamma = 29.3$, ω_D is completely independent of E. Consequently, by working at the so-called "magic" value of γ, $\gamma = 29.3$, it is possible to use electric fields for focusing without affecting ω_D. A weak-focusing storage ring can be designed which incorporates a uniform magnetic field and an electric quadrupole field. Because of the uniform magnetic field, precise knowledge of the radial distribution of the stored particles is not necessary. For muons, the magic energy is approximately 3 GeV.[23] An experiment at this energy incorporating an electrostatically focused storage ring with a uniform magnetic field (11 kG) is currently under construction at CERN. The radius of the ring is 7 m. The projected accuracy is approximately 10 ppm of a_μ.

The muon physics group at Yale has proposed a similar experiment using 1 GeV muons ($\gamma \cong 10$). Even for values of γ other than 29.3, it is possible to achieve weak focusing with a suitable combination of inhomogeneous electric and magnetic fields, and, at the same time, make ω_D essentially independent of the radius of the stored muon. The proposed experiment features a small superconducting storage ring ($B \cong 40$ kG, $r \cong 1$ m). The lower value of γ means that the increase in accuracy due to time-dilation (see Sec. 3.1.4) will be considerably smaller than in the new CERN experiment. However, the higher magnetic field more than offsets the effect of the lower value of γ (the product $B\gamma$ is a useful figure of merit for muon experiments). The projected overall accuracy is 10–20 ppm of a_μ.

In view of the two proposed muon experiments, it appears probable that a 10 ppm determination of a_μ will become available in the next few years. If so, the uncertainties in theory and experiment will be of similar magnitude, and it may then be possible to test some of the current speculations on the effects of strong interactions on the muon anomaly.

4.4 Conclusions

The experimental discovery (1947) that the electron g-factor differed from the Dirac "2" was one of the key experiments which ushered in quantum electrodynamics as we know it. Since this early period there have been continuous point-counterpoint comparisons of theory and experiment, until today the level of accuracy of the comparisons has reached 3 ppm for the electron anomaly, 300 and 700 ppm, respectively, for the negative and positive muon anomalies, and 1000 ppm for the positron anomaly.

The theoretical calculations are now all in agreement with their respective experiments to within about one standard deviation. This agreement constitutes the cleanest and most precise verification of the theoretical

[23] The magic energy for electrons is 14 MeV. In principle, this would solve the electric field problems encountered in the electron precession experiments. However, for a magnetic mirror trap, energy loss due to synchrotron radiation is prohibitive. A storage-ring experiment incorporating an accelerating cavity might be feasible.

structure and calculational procedure of quantum electrodynamics yet devised.

Is yet further refinement of theory and experiment possible? If so, is this indeed a reasonably fruitful area in which to look for breakdowns of QED or for an answer to the muon–electron puzzle? Alternatively, does anchoring the theory firmly to higher and higher order really improve our understanding of the leptons and their vacuum interactions at a level in any way commensurate with the effort involved?

The first question has been dealt with explicitly in Secs. 4.1–4.3, as well as throughout the text. The answer is that, very broadly speaking, better than order of magnitude increases in accuracy are probably possible in the experimental values of a_μ and a_e using extensions of existing techniques. We point out that if, in particular, such an electron experiment is successful, an equal increase in the accuracy of the theoretical calculation of a_e and in knowledge of the fine structure constant will be necessary if a meaningful comparison is to be made. Since a_μ has already been calculated to about fifteen times the current experimental accuracy no such increase is required for the muon.

Unfortunately the second question cannot be so definitively answered. There is to our knowledge no theory which has been advanced as an alternative to, or extension of, quantum electrodynamics and which makes explicit predictions which are different from those of QED. We do not include here the various "breakdowns" discussed in Sec. 2.2. None of these makes compelling new predictions which are independent of arbitrary parameters; parameters that are to be fit *after* a breakdown is discovered experimentally. However, the history of physics indicates that successful new theories often arise from small deviations in details of the preceding theory. With this in mind, and in the absence of theory or experiment indicating a specific lack of sensitivity of g-2 to a breakdown of QED, tests to still higher accuracy appear to be as fruitful a method as any for investigating the structure of the theory.

ACKNOWLEDGMENTS

The Michigan g-2 Experiments have been generously supported by the U.S. Atomic Energy Commission under Contract AT(11–1) 1112. One of us (A.R.) also thanks the National Bureau of Standards for a *Precision Measurements Grant* which has been most helpful in the preparation of this paper.

We thank Professor S. Brodsky, Professor G. W. Ford and Professor Y. K. Yao for their help and comments on the material of Sec. II. We also thank Professor Ford and Miss S. Granger for making their unpublished spin calculations available to us. Finally we acknowledge the useful and detailed comments of the referees.

REFERENCES

Aldins, J., T. Kinoshita, S. J. Brodsky, and A. Dufner, 1970, Phys. Rev. **D1,** 2378.
Bailey, J., W. Bartel, G. von Bochman, R. C. A. Brown, F. J. M. Farley, H. Jöstlein, E. Picasso, and R. W. Williams, 1968, Phys. Letters **28B,** 287.
——, and E. Picasso, 1970, Prog. Nucl. Phys. **12,** 43.
——, 1968, Proc. XIV Int. Conf. on High Energy Physics, Vienna.
Bargmann, V., L. Michel, and V. L. Telegdi, 1959, Phys. Rev. Letters **2,** 435.
Barber, W. C., B. Gittelman, G. K. O'Neill, and B. Richter, 1966, Phys. Rev. Letters **16,** 1127.
——, 1961, Sov. Phys. JETP **12,** 993.
Berestetskij, V. B., O. N. Krokhin, and A. K. Khlebnikov, 1956, Zurn. Eksp. Teor. Fiz. **30,** 788.
Bethe, H., 1947, Phys. Rev. **72,** 339.
Bloch, F., 1953, Physica **19,** 821.
Bloom, M., and K. Erdman, 1962, Can. J. Phys. **40,** 179.
Breit, G., 1947, Phys. Rev. **72,** 984.
——, 1948, Phys. Rev. **73,** 1410.
——, 1948, Phys. Rev. **74,** 656.
Brodsky, and S. D. Drell, 1970, Ann. Rev. Nuclear Science, **20,** 147.
——, and T. Kinoshita, 1970, *Theoretical Results for Sixth Order Contributions to the Anomalous Magnetic Moment of the Muon and Electron*, submitted to the XVth Intern. Conf. on High Energy Physics, Kiev.
——, and J. D. Sullivan, 1967, Phys. Rev. **156,** 1644.
Burnett, T., and M. J. Levine, 1967, Phys. Letters, **24B,** 467.
Byrne, J., 1963, Can. J. Phys. **41,** 1571.
Charpak, G., F. J. M. Farley, R. L. Garwin, T. Muller, J. C. Sens, V. L. Telegdi, and A. Zichichi, 1961, Phys. Rev. Letters **6,** 128.
——, F. J. M. Farley, R. L. Garwin, T. Muller, J. C. Sens, and A. Zichichi, 1962, Phys. Letters **1,** 16.
——, F. J. M. Farley, R. L. Garwin, T. Muller, J. C. Sens, and A. Zichichi, 1965, Nuovo Cimento **37,** 1241.
Cisneros, A., 1970, Astrophysics and Space Science 10, 87.
Coffin, T., R. L. Garwin, L. M. Lederman, and A. M. Sachs, 1958, Phys. Rev. **109,** 973.
Compton, A. H., 1921, J. Franklin Institute **192,** 145. See also: Kennard, E. H., 1922, Phys. Rev. **19,** 420.
Corben, H. C., 1968, *Classical and Quantum Theories of Spinning Particles*, (Holden-Day, San Francisco).
Dehmelt, H. G., 1958, Phys. Rev. **109,** 381.
——, and F. L. Walls, 1968, Phys. Rev. Letters **21,** 127.
Dirac, P. A. M., 1927, Proc. Roy. Soc. (London) **A117,** 610.
——, 1928, Proc. Roy. Soc. (London) **A118,** 351.
——, 1957, *The Principles of Quantum Mechanics*, (Oxford U. P., London, 4th ed.)
Drell, S. D., and H. R. Pagels, 1965, Phys. Rev. **140,** B397.
Dyson, F. J., 1949, Phys. Rev. **75,** 486.
——, 1949, Phys. Rev. **75,** 1736.
Farago, P. S., 1965, Adv. in Electronics and Electron Physics, **21,** 1.
——, R. B. Gardiner, J. Muir, and A. G. A. Rae, 1963, Proc. Phys. Soc. (London) **3,** 82, 493.
Farley, F. J. M., 1968, Cargese Lectures in Physics, edited by M. Levy (Gordon and Breach, New York), Vol. 2.
——, 1969, Nuovo Cimento **1,** 59.
——, J. Bailey, R. C. A. Brown, M. Giesch, H. Jöstlein, S. Van der Meer, E. Picasso, and M. Tannenbaum, 1966, Nuovo Cimento **44,** 281.
Feynman, R. P., 1948, Rev. Mod. Phys. **20,** 367.
——, 1948, Phys. Rev. **74,** 1439.
——, 1961, *Quantum Electrodynamics* (Benjamin, New York).
Fierz, M., and V. L. Telegdi, 1970, *Quanta*, edited by Goebel and Nambu, (University of Chicago Press), p. 209.
Ford, G. W., and C. W. Hirt, 1961, University of Michigan, Contract No. NONR 1224(15) (unpublished report).
Franken, P. A., and S. Liebes, Jr., 1956, Phys. Rev. **104,** 1197.
Gardner, J. H., and E. M. Purcell, 1949, Phys. Rev. **76,** 1262.
——, 1951, Phys. Rev. **83,** 1951.
Gilleland, J. and A. Rich, 1969, Phys. Rev. Letters **23,** 1130.
Gourdin, M. and E. de Raphael, 1969, Nucl. Phys. **B10,** 667.
Gräff, G., F. G. Major, R. W. H. Roeder, and G. Werth, 1968, Phys. Rev. Letters **21,** 340.

——, E. Klempt and G. Werth, 1969, Z. Physik **222,** 201.
Hardy, W. A., and E. M. Purcell, (private communication, E. M. Purcell).
Hearn, A. C., Stanford University Report No. ITP-247, and in *Interactive Systems for Experimental Applied Mathematics*, edited by M. Klerer and J. Reinfelds (Academic, New York, 1968).
Henry, G. R., and J. E. Silver, 1969, Phys. Rev. **180,** 1262.
Hughes, V. W., Proposed submitted to LAMPF, Yale University, March 1971.
Hutchinson, D. P., F. L. Larsen, N. C. Schoen, D. I. Sober, and A. S. Kanofsky, 1970, Phys. Rev. Letters **24,** 1254.
Karplus, R., and N. Kroll, 1950, Phys. Rev. **77,** 536.
Kennard, E. H., 1922, Phys. Rev. **19,** 420.
Koba, Z., 1949, Prog. Theoret. Phys. **4,** 319.
Kincaid, B., 1970, private communication.
Klein, E., 1968, Z. Physik **208,** 28.
Knight, L. V., 1965, Ph.D. thesis, Stanford Univ., unpublished.
Kramers, H. A., 1957, *Quantum Mechanics* (North Holland, Publ. Co., Amsterdam).
Kroll, N., 1966, Nuovo Cimento, **45A,** 65.
Kusch, P., and H. M. Foley, 1947, Phys. Rev. **72,** 1256.
——, and H. M. Foley, 1947, Phys. Rev. **73,** 412.
——, and H. M. Foley, 1948, Phys. Rev. **74,** 250.
Lamb, W. E., and R. C. Retherford, 1947, Phys. Rev. **72,** 241.
Lautrup, B. E., and E. de Rafael, 1968, Phys. Rev. **174,** 1835.
——, A. Petermann, and E. de Rafael, 1971, Physics Reports (to be published).
Lee, T. D., and G. C. Wick, 1969, Nucl. Phys. **B9,** 209.
Levine, M. J., and Wright, J., 1971, Phys. Rev. Letters **26,** 1351.
Louisell, W. H., R. W. Pidd, and H. R. Crane, 1953, Phys. Rev. **91,** 475.
——, R. W. Pidd, and H. R. Crane, 1954, Phys. Rev. **94,** 7.
Luttinger, J., 1948, Phys. Rev. **74,** 893.
Mendlowitz, H., and K. M. Case, 1955, Phys. Rev. **97,** 33.
Mignaco, J. A., and E. Remiddi, 1969, Nuovo Cimento **60A,** 1519.
Mott, N. F., and H. S. W. Massey, 1965, *Theory of Atomic Collisions* (Oxford U. P., London) p. 214–218.
Nafe, J. E., E. B. Nelson, and I. I. Rabi, 1947, Phys. Rev. **71,** 914.
Parsons, R. G., 1968, Phys. Rev. **168,** 1562.
Pauli, W., 1933, *Handbuch der Physik* (Springer-Verlag, Berlin), Vol. **24,** Part 1, p. 242.
Petermann, A., 1957, Helv. Phys. Acta **30,** 407.
——, 1957, Phys. Rev. **105,** 1931.
Rastall, P., 1962, Can. J. Phys. **40,** 1271.
Rich, A., and H. R. Crane, 1966, Phys. Rev. Letters **17,** 271.
——, 1968, *Proceedings of the Third International Conference on Atomic Masses, and Related Constants*, edited by R. C. Barber, (Manitoba U. P., Winnipeg, Canada.)
——, 1968, Phys. Rev. Letters **20,** 967; see also F. J. M. Farley, 1968, in *Cargese Lectures in Physics*, edited by M. Levy (Gordon and Breach, New York), Vol. 2.
Ruderman, M. A., 1966, Phys. Rev. Letters **17,** 794.
Sandars, P. G. H., and E. Lipworth, 1964, Phys. Rev. Letters **13,** 718.
Schwinger, J. S., 1947, Phys. Rev. **73,** 416.
——, 1948, Phys. Rev. **74,** 1439.
——, 1949, Phys. Rev. **75,** 651.
——, 1949, Phys. Rev. **76,** 790.
Schupp, A. A., R. W. Pidd, and H. R. Crane, 1961, Phys. Rev. **121,** 1.
Sokolov, A. A., and I. G. Pavlenko, 1967, Optics and Spectroscopy **22,** 1.
Sommerfield, C. M., 1957, Phys. Rev. **107,** 328.
——, 1957, Ann. Phys. **5,** 26.
Suura, H., and E. H. Wichmann, 1957, Phys. Rev. **105,** 1930.
Taylor, B. N., W. H. Parker, and D. N. Langenberg, 1969, Rev. Mod. Phys. **41,** 375.
Tomonaga, S., 1946, Prog. Theor. Phys. **1,** 27; (see Dyson, 1949, for a complete summary of references).
Uhlenbeck, G. E., and S. Goudsmit, 1925, Naturewiss. **47,** 953.
——, 1926, Nature **117,** 264.
Walls, F. L., 1970, Ph.D. thesis, Univ. of Washington (unpublished).
Welton, T. A., 1948, Phys. Rev. **74,** 1157.
Wesley, J. C., 1970, Ph.D. thesis, University of Mich. (unpublished).
——, and A. Rich, 1970, Phys. Rev. Letters **24,** 1320.
——, and A. Rich, 1971, Phys. Rev. **A4,** 1341.
Wilkinson, D. T., and H. R. Crane, 1963, Phys. Rev. **130,** 852.